Ecological Economics 209 (2023) 107800

Contents lists available at ScienceDirect

Ecological Economics

journal homepage: www.elsevier.com/locate/ecolecon

The effect of pests and pathogens on forest harvesting regimes: A bioeconomic model

Ewan McTaggart [a,*], Itamar Megiddo [b], Adam Kleczkowski [a]

[a] Department of Mathematics & Statistics, University of Strathclyde, Glasgow, UK
[b] Department of Management Science, University of Strathclyde, Glasgow, UK

ARTICLE INFO

Keywords:
Bioeconomic modelling
Forest management
Tree pathogens and diseases
Schaefer–Faustmann model
Optimal thinning and rotation
Optimal harvesting

ABSTRACT

Pests and diseases are an existential threat to trees in forests and woodlands. There is, therefore, a pressing need to use ecological and bioeconomic models to inform forest managers on control and mitigation strategies. For example, the incidence of Dothistroma needle blight in the UK has increased rapidly since the 1990s, and it is a significant threat to the productivity of commercial forestry. Climatic changes are expected to exacerbate this problem further. Control of the disease in the UK primarily focuses on good stand management through pre-commercial thinning; similar practices are widely used in commercial forests worldwide. Forest managers would benefit from evidence on the effectiveness of this precautionary strategy (in comparison to its alternatives) to reduce disease impacts and increase the value extracted from timber. In this paper, we develop a bioeconomic model to determine the economically optimal harvesting regime – in terms of thinning and rotation – of an even-aged plantation under the risk of an invading pest. We extend a Schaefer–Faustmann model to include a compartmental epidemiological system that governs timber growth and disease spread. We analyse a set of management regimes, including the timing of the final clear-felling of the forest and the timing and level of earlier thinning. Thus, in our approach, forest managers decide whether and when to thin and must balance (i) harvesting before infection destroys the timber's value and (ii) exploiting the forest's density-dependent growth. We use a sensitivity analysis with respect to the disease spread and impact on the tree dynamics to demonstrate that, in the presence of disease, thinning can significantly improve the net present value of the plantation if applied correctly. Furthermore, if thinning reduces the transmission rate significantly, the priority is to protect the final harvest, and rotations extend while the thinning time shortens. Our study provides a framework to help design appropriate forest management strategies in the presence of disease.

1. Introduction

Outbreaks of invasive pests and pathogens disrupt forest services and cause significant ecological, economic, and social losses (Roberts et al., 2020; Boyd et al., 2013). The incidence of such outbreaks worldwide has grown with the globalisation of trade and climatic changes (Ramsfield et al., 2016) — a trend expected to continue (Sturrock et al., 2011). In the last few decades, the arrival and establishment of Chalara ash dieback (*Hymenoscyphus fraxineus*), European spruce bark beetle (*Ips typographus*) and Dothistroma needle blight (*Dothistroma septosporum*) has stressed UK forests (Marzano et al., 2017; Forestry Commission, 2012; Freer-Smith and Webber, 2017). These pests could devastate the flow of woodland ecosystem services, which contribute £3.3 billion to the UK economy annually (Office for National Statistics, 2020). In this paper, we consider a commercial forest where the manager is interested in minimising economic losses due to disease in terms of the timber benefit. We investigate how the optimal harvesting strategy – in terms of thinning and rotation – changes under the risk of an invading pest.

For some diseases, the focus is on arrival prevention in the UK, and for others, it is on early detection, eradication or containment to prevent economic impacts and loss of valued habitats and landscapes (Marzano et al., 2017). In many cases, eradication of pests or pathogens after their detection, through measures such as widespread clear-felling or chemical treatment, is not an option (Roberts et al., 2020; Klapwijk et al., 2016; Potter and Urquhart, 2017). Management options revolve around mitigation to reduce disease impacts, and secondary infection pathways (Roberts et al., 2020). Silvicultural practices such as diseased tree removal, changing species after rotation, pruning, coppicing, and thinning are deployed (Roberts et al., 2020). In this

* Corresponding author.
E-mail address: ewan.mctaggart@strath.ac.uk (E. McTaggart).

https://doi.org/10.1016/j.ecolecon.2023.107800
Received 9 September 2022; Received in revised form 30 January 2023; Accepted 2 March 2023
Available online 31 March 2023

paper, we consider thinning and clear-felling as the two options for the plantation, after which the land lays bare.

In established stands, thinning is the primary method of influencing the growth and development of trees (Kerr and Haufe, 2011). Leaving forests unthinned would lead to the premature mortality of trees due to competition for light and other resources (Matthews et al., 2016). Whereas, thinning frees up growing space and reduces this competition among closely spaced stems, accelerating the growth of the remaining trees (Forestry Commission, 2015). This allows forest managers to achieve target merchantable products (in terms of tree diameters and stand uniformity) and increases the value of timber extracted at rotation (Zeide, 2001).

Thinning a stand can manipulate environmental conditions to diminish secondary infection pathways (Roberts et al., 2020), and can also increase the resilience of the remaining trees to diseases (reducing the stress on trees, leading to healthier and stronger trees less susceptible to diseases) (Boyle et al., 2016). In the UK, control of Dothistroma Needle Blight focuses on good stand management and "learning to live with the disease" (Bulman et al., 2016; Quine et al., 2014). This includes thinning to improve airflow and make conditions less conducive to fungus development (Forest Research, 2022a). Thinning increases the distance between trees (reducing tree density) and reduces the effectiveness of rain-splashed spores (Bulman et al., 2016). After a chemical treatment in response to spruce budworm outbreak, thinning may be used to increase tree and stand resistance to the pest through increased foliage production (Bauce and Fuentealba, 2013). Similarly, thinning acts as a preventative tactic for bark beetles by improving tree vigour (Hlásny et al., 2019).

Ecological and bioeconomic models that explore thinning as a forest management strategy are largely based on the classic Faustmann model (Martin Faustmann, 1849) (Samuelson, 1976). The Faustmann model is a net present value (NPV) framework that determines the optimal rotation age for an even-aged stand under the assumption of periodical regeneration and rotation. One approach that explores a thinning strategy operates at the tree level and determines individual tree harvesting times within a forest (Coordes, 2014). In another approach, Clark and De Pree (1979) let the growth of the total timber stock in the Faustmann model react to annual harvests, becoming a Schaefer–Faustmann model. They analysed this model with optimal control to show that optimal annual thinning follows a bang–bang strategy (Clark and De Pree, 1979). Halbritter and Deegen (2015) build on this and perform a deterministic analysis of the combined optimal planting density, thinning and rotation for an even-aged stand. Similarly, Tahvonen (2016) adapts (Clark and De Pree, 1979) to investigate the conditions under which continuous cover production forestry is optimal in place of rotation forestry.

The Faustmann model has also been extended to consider disease risk. Reed (1984) first explored the impact of natural disturbances on optimal forest management (rotation length and net present value). He adapted the infinite rotation Faustmann formula to include the risk of catastrophic loss from wildfires with a homogeneous Poisson distribution. However, as Macpherson et al. (2016, 2017a,b) argue, tree diseases exhibit key differences compared to other natural disturbances like storms or wildfires, and models should account for these. In particular, disease progresses at a slower speed. While it can progress at variable time scales, the likely units are years. Further, the symptoms (cryptic infection) can result in the disease remaining undetected for long periods. Lastly, the long-term persistence of many pathogens following their invasion is often irreversible. Given these differences, Macpherson et al. (2016, 2017a,b) link a single rotation NPV framework/Faustmann model to a deterministic susceptible-infected compartmental model, to estimate pest/pathogen density impact on impact timber revenue. They investigate the effect of disease on the optimal rotation length (with Macpherson et al., 2017a and without Macpherson et al., 2016 the inclusion of non-timber benefits attributed to the forest) and the optimal mix of planted species (Macpherson et al., 2017b). An et al. (2019) recently adapted the Macpherson framework and used a structural damage function (a generalised linear model with probit link function, from Cobourn et al., 2011) to capture disease dynamics and their impact. They find the optimal rotation age when pest damage depends on their density and climatic variables, and predict Pine Wilt disease's damage rate and economic impact under different disease conditions, climate scenarios, and interventions.

Models that build on the Faustmann Model to integrate disease (or natural disasters) and thinning capture some of the interactions between tree growth, thinning, and outbreak progression/risk. Halbritter et al. (2020) accompany a Schaefer–Faustmann model (Halbritter and Deegen, 2015) with an age and density-dependent hazard function to represent the arrival of catastrophic natural risks (fire, storms, pests). Using optimal control theory, they analytically explore the optimal annual thinning regime and rotation length under different risks, interest rates, and timber prices. Petucco and Andrés-Domenech (2018) extend the Faustmann model by adding a fixed thinning regime and considering the combined impact of storms and a defoliator pest (Pine Processionary Moth). Their timber growth model accounts for the number of trees, their heights, and the basal area. These factors are impacted in unique ways by windstorms (modelled as random Poisson events) and the annual pest density (given by a sinusoidal statistical model). Thinning has no effect on the frequency or severity of any of the risks. Although Petucco et al. do not optimise thinning, they investigate how these disturbances change the optimal rotation length and the land's expectation value. Staupendahl and Möhring (2011) model an even-aged spruce stand with fixed pre-commercial thinning intervals, and estimate the optimal rotation length and annuity under risk (under the assumption of infinite rotations). They use an exogenous age-dependent survival function (Weibull distribution) to model the area of forest remaining after damage from "natural risks" (storms or pests) and perform a sensitivity analysis to different risk distributions.

In this paper, we develop a bioeconomic model to determine economically optimal harvesting regimes – in terms of thinning and rotation – of an even-aged plantation under the risk of an invading pest. We extend a Schaefer–Faustmann model (Tahvonen, 2016) to include a compartmental epidemiological system that governs timber production and disease spread/dynamics. Using a dynamic compartmental model of disease separates our approach from previous bioeconomic studies that considered thinning and disease (Halbritter et al., 2020; Petucco and Andrés-Domenech, 2018; Staupendahl and Möhring, 2011), while expanding the Macpherson et al. framework (Macpherson et al., 2016, 2017a,b) to include thinning. The compartmental model can represent diseases that are unique from catastrophic events in their speed of progression, symptoms, and management response when detected (Macpherson et al., 2016). Furthermore, it allows for interactions between thinning, tree growth and disease progression. We consider thinning's effect on both forest growth and disease spread: it increases growth by reducing the forest volume and thus reducing competition between trees; it reduces pest or pathogen spread by increasing the space and airflow between trees and tree resilience e.g., with *Dothistroma septosporum* (Roberts et al., 2020). Thinning and rotation thus effect both forest growth and disease dynamics. We provide insight into the system dynamics and sensitivity to key parameters (controlling infection spread rate secondary and severity/impact). Furthermore, we optimise the thinning timing and intensity during the rotation (unlike (Petucco and Andrés-Domenech, 2018; Staupendahl and Möhring, 2011)), and explore the optimal strategy — particularly the role of thinning.

This paper is structured as follows. In Section 2 we detail the general economic model and the underlying epidemiological system. The results corresponding to our model are given in Section 3, and discussed in Section 4. We give our concluding remarks in Section 5.

Table 1
Parameter definitions, alongside their base case values.

Parameter	Description	Base case value[a]
ECOLOGICAL		
T_F	Rotation length/clear-felling time (years)	88.74[b]
T_1	Thinning time (years)	60.40[c]
γ	Proportion of trees thinned/thinning intensity	0.74[d]
t	Time (years)	
$g(t)$	Age-dependent growth increment	$0.13e^{-0.01t}$
K	Carrying capacity of plot	378
EPIDEMIOLOGICAL		
$x(t)$	Susceptible (uninfected) timber volume (m^3)	
$y(t)$	Infected timber volume (m^3)	
$B(t)$	Transmission rate ($m^{-3}ha^{-1}t^{-1}$)	Eq. (3)
β	Initial transmission rate ($m^{-3}ha^{-1}t^{-1}$)	0.004
P	Primary infection rate ($ha^{-1}t^{-1}$)	0.0003
ϵ	Growth of infected timber relative to uninfected timber	1
δ	Impact of thinning on transmission rate	0
ECONOMIC		
$\hat{J}$	Net Present Value, NPV ($£ha^{-1}$)	3.34
p_1	Price of uninfected thinned timber ($£m^{-3}$)	30.87
p_2	Price of uninfected clear-felled timber ($£m^{-3}$)	30.87
r	Discount rate	0.03
W_p	Establishment cost ($£ha^{-1}$)	1000
ρ	Revenue from a unit of infected timber relative to uninfected timber	1

The base case values (a) represent a model without disease ($\epsilon = \rho = 1$). The management variables (b) (c) (d) are the corresponding optimal strategy in a thinning and rotation regime (solving Eq. (7) for the base case values) — the "disease-free" strategy. The age-dependent growth increment, $g(t)$, was adapted from the numerical example in Tahvonen (2016). The establishment cost W_p comes from the same source. The timber prices p_1, p_2 are assumed equal and were taken from the Coniferous Standing Sales UK Price Index (Braby, 2022).

2. Model framework

We build on a Schaefer–Faustmann model (Tahvonen, 2016) to determine the economically optimal harvesting regime – in terms of thinning and rotation – of an even-aged plantation under the risk of an invading pest. The model depends on a compartmental system that governs timber production and disease dynamics. Disease impact on the stands value is included by scaling the revenue obtained from the timber of infected trees or the growth of infected trees. Our timber production model is age and density-dependent, and operates at the stand volume level. It captures thinning reduces the volume of the forest, thinning resulting in increased tree growth (by lowering competition between trees), and thinning can reduce the spread of a pest or pathogen.

In the first subsection, we introduce this ecological system governing timber production and disease dynamics. In the following subsection, we derive the maximisation problems to optimise management regimes for the plot. All relevant parameter definitions for the applied model are in Table 1.

2.1. Forest dynamics — the compartmental timber production model

We now develop the two-state compartmental model of forest dynamics. We use Dothistroma needle blight, a foliar disease caused by the fungal pathogen *Dothistroma septosporum* (Mullett et al., 2016), as an example to build the model. However, the assumptions we make are generic enough to represent other tree diseases with similar effects.

We compartmentalise timber on a hectare of even-aged monoculture into two states of infection ($N = 2$), infected with Dothistroma needle blight or not. We let $x(t) \geq 0$ and $y(t) \geq 0$ be the susceptible and infected stand volumes (m^3ha^{-1}). Initially bare land is purchased and susceptible trees planted, with $x(0) = 1$ and $y(0) = 0$. The following (Susceptible-Infected) system governs the evolution of timber volumes in each state,

$$\begin{aligned} \frac{dx}{dt} &= g(t)x\left(1-\frac{(x+y)}{K}\right) - h(t)x - (P + B(t)y)\,x \\ \frac{dy}{dt} &= \epsilon g(t)y\left(1-\frac{(x+y)}{K}\right) - h(t)y + (P + B(t)y)\,x. \end{aligned} \tag{1}$$

We assume generally that the annual growth increment for timber in each state is the product of an age-dependent function $g(t)$ and a density/volume-dependent function as in Clark and De Pree (1979), Halbritter and Deegen (2015) and Tahvonen (2016). Furthermore, the infected timber growth increment is multiplied by a constant ϵ to represent reduced growth from infection. The age-dependent function, $g(t)$, is positive and decreasing with time, representing the growth potential of a stand decreasing with age. The density-dependent growth function is a concave down quadratic with respect to the total forest volume (Halbritter and Deegen, 2015; Tahvonen, 2016). When competition (timber volume) is high, tree growth is limited, and reducing density can increase growth (Forestry Commission, 2015).

Specifically, we assume susceptible timber grows annually at a rate of $g(t)(1-\frac{x+y}{K})$, which we adapted from the numerical example in Tahvonen (2016) modelling the growth of Norway Spruce. Norway Spruce is susceptible to Dothistroma needle blight (DNB), but the susceptibility is low and requires high infection pressure (Forest Research, 2022b). The carrying capacity of the plot is K (m^3). We assume infected timber grows at the same rate as susceptible if $\epsilon = 1$ and at a scaled rate if $0 < \epsilon < 1$. Furthermore, if $\epsilon = 1$, the total annual growth of all timber equals the age-dependent effect $g(t)$ multiplied by a total density/volume-dependent effect $(x+y)\left(1-\frac{x+y}{K}\right)$, similarly to Clark and De Pree (1979), Tahvonen (2016) and Halbritter and Deegen (2015). We selected the functions $g(t)$ and $(1-\frac{x+y}{K})$ so growth represents plantation forestry. They result in logistic growth which tends to zero independently of stand density. After a clear-felling the volume does not grow back, but after a thinning it recovers. This represents the

remaining trees after thinning (which reduces forest density) experiencing increased growth, resulting in larger diameters (Mäkinen and Isomäki, 2004).

Susceptible timber becomes infected with primary infection rate P. This represents external infection pressure, such as long range dispersal of spores in clouds or mist, or by movement of infected planting stock (Scottish Forestry). Within a forest containing infection, spread occurs primarily during periods of damp weather, which is conducive to fungal spore production. Spores are spread between trees by rain splashes and wind (Scottish Forestry; Mullett et al., 2016). Forest Research states that in the UK, control of the disease typically involves planting resistant species after rotation, and good stand management. In particular, this includes thinning in accordance with good silvicultural practice, to improve air flow and make conditions less conducive to fungus development (Forest Research, 2022a). Thinning also increases the distance between trees and, thus, reduces the effectiveness of rain-splashed spores (Bulman et al., 2016). Therefore, we assume that thinning removes a proportion of trees indiscriminately of their infection state. This assumption is reasonable for other diseases for which detection of infection is costly/difficult or the trees exhibit few outward signs of the disease until the later stages of infection. We denote the proportion of timber volume harvested per hectare per year ($m^3 ha^{-1} t^{-1}$) by $h(t)$, with

$$h(t) = \begin{cases} \gamma, & t = T_1 \\ 1, & t = T_F \\ 0, & \text{otherwise.} \end{cases} \tag{2}$$

We assume that a single thinning occurs (instead of annual (Tahvonen, 2016)) at time $T_1 \geq 0$ and $\gamma \in [0, 1)$ of the total timber volume is removed, indiscriminate of its infection state. After T_F years, the plot is clear-felled ($x_i(t) = 0$ for $t > T_F$) and lays bare.

We also assume that the transmission (secondary infection) rate, $B(t)$, which controls the spread of disease within the forest, is a step function,

$$B(t) = \begin{cases} \beta, & t \leq T_1 \\ \beta e^{-\delta\gamma}, & t > T_1. \end{cases} \tag{3}$$

The transmission rate is initially β. Thinning at $t = T_1$ can reduce the transmission rate, with the strength of this thinning effect determined by the factor $\delta \geq 0$. If there is an effect ($\delta > 0$), its impact increases with the proportion of trees thinned (γ). We assume a density-dependent transmission term (Kleczkowski et al., 2019) in Eq. (1), and therefore increased total forest volume (and therefore density in our model) results in increased spread within the forest.

2.2. Economic model

We now develop the single rotation Schaefer–Faustmann model for the even-aged forest, where the NPV includes the establishment cost, and the benefits from harvesting the timber. Initially, a hectare-sized plot is purchased and susceptible trees are planted, amounting to W_p (£'s) in establishment costs. Thinning at T_1 and clear-felling at T_F produces the timber benefits $H_{T_1}(\gamma, T_1)$ and $H_{T_F}(\gamma, T_1, T_F)$, both measured in £'s. After clear-felling, the land lays bare ($x(t) = y(t) = 0$ for $t > T_F$). We discount the revenue from harvesting at the rate r. Therefore, the NPV of the plot (the objective function) is

$$\hat{J}(\mathbf{s}) = -W_p + H_{T_1}(\gamma, T_1) e^{-rT_1} + H_{T_F}(\gamma, T_1, T_F) e^{-rT_F}, \tag{4}$$

where $\mathbf{s} = (\gamma, T_1, T_F)$.

Let p_1 and p_2 be the constant prices (£'s per m^3) for thinned and clear-felled susceptible timber, respectively. Assume $p_1 \leq p_2$: thinned timber is generally not as mature and therefore valuable as when clear-felled. Following the approach by Macpherson et al. (2016, 2017b), we assume that the disease causes a reduction in the value of timber (e.g., through reduced quality or yield). In particular, DNB causes defoliation of the needles of an infected tree. This gradually weakens the tree, significantly reducing timber yields and eventually causing mortality (Forest Research, 2022a). Therefore, we let ρ be the revenue from a unit of infected timber relative to susceptible timber, where $0 \leq \rho \leq 1$.

We write the benefit from harvested timber in the each state as the product of the price per m^3 of standing timber, the volume of timber produced, and if timber is infected, then also the scaling parameter ρ. Therefore, the total timber benefit from thinning at T_1 is

$$\begin{aligned} H_{T_1}(\gamma, T_1) &= p_1 h(T_1) x(T_1) + p_1 h(T_1) \rho y(T_1) \\ &= p_1 \gamma \left\{ x(T_1) + \rho y(T_1) \right\}, \end{aligned} \tag{5}$$

and the total timber benefit at the rotation time, T_F, is

$$\begin{aligned} H_{T_F}(\gamma, T_1, T_F) &= p_2 h(T_F) x(T_F) + p_2 h(T_F) \rho y(T_F) \\ &= p_2 \left\{ x(T_F) + \rho y(T_F) \right\}. \end{aligned} \tag{6}$$

Where Eq. (6) is a function of thinning proportion (γ) and time (T_1) because the volumes at rotation, $x(T_F)$ and $y(T_F)$, depend on these variables.

The forest manager's task is to maximise the NPV of the stand over a single rotation. We investigate two different management regimes. The first is thinning and rotation, where a single thinning occurs before clear-felling. There are three control variables; the thinning time (T_1), thinning proportion (γ), and rotation length (T_F). Their optimal values that maximise the objective function Eq. (4) are given by

$$\begin{aligned} \mathbf{s}^*_{tr} = \arg\max_{\mathbf{s}} \quad & \hat{J}(\mathbf{s}), \quad \text{where} \quad \mathbf{s} = (\gamma, T_1, T_F) \\ \text{subject to} \quad & \gamma \in [0, 1) \\ & T_F \geq T_1 \geq 0 \end{aligned} \tag{7}$$

The second management regime is rotation only, a Faustmann model. The maximisation problem is choosing the rotation length that maximises the NPV, as explored by Macpherson et al. (2016). The optimal strategy is

$$\mathbf{s}^*_r = \arg\max_{T_F \geq 0} \hat{J}(\mathbf{s}), \quad \text{where} \quad \mathbf{s} = (0, 0, T_F) \tag{8}$$

We solved the optimisations problems Eqs. (7) and (8) numerically in R using the Optim package and the L-BFGS-B algorithm. For Eq. (7) we ran the algorithm with three different start points and chose the best solution.

3. Results

We compare the optimal management strategies without disease in Section 3.1. In Section 3.2 we introduce disease, and in its first two subsections, we let susceptible and infected timber growth be the same ($\varepsilon = 1$), and assume that thinning does not effect transmission ($\delta = 0$). We first compare optimal management strategies for the case with no revenue from infected timber ($\rho = 0$) in Section 3.2.1. Sensitivity analysis of the revenue from a unit of infected timber relative to susceptible (i.e., $\rho > 0$) is undertaken in Section 3.2.2. Finally, we introduce and investigate the impact of the thinning effect ($\delta > 0$) and the reduction in infected timber growth ($\varepsilon < 1$) on the optimal strategy, Section 3.2.3.

To guide our intuition for these future sections, we will first find the optimal rotation length that maximises the NPV Eq. (4), assuming that the thinning proportion (γ) and time (T_1) are fixed. We derive the first order condition by differentiating Eq. (4) with respect to T_F,

$$\frac{\partial \hat{J}}{\partial T_F} = p_2 \left\{ x'(T_F) + \rho y'(T_F) \right\} e^{-rT_F} - r p_2 \left\{ x(T_F) + \rho y(T_F) \right\} e^{-rT_F}. \tag{9}$$

Setting Eq. (9) equal to zero and rearranging gives the optimal rotation length condition

$$p_2 x'(T_F) + \rho p_2 y'(T_F) = r p_2 \left\{ x(T_F) + \rho y(T_F) \right\}. \tag{10}$$

The optimal rotation length, T_F, which satisfies the above is the point when the rate of return of timber production equals the opportunity cost (rate of return of clear-felling and storing cash in the bank). We can show the rotation length T_F that satisfies this condition, Eq. (10), is a maximum by plotting the NPV as a function of T_F. Furthermore, by substitution of $x'(T_F)$ and $y'(T_F)$ from Eq. (1) into Eq. (10) and rearranging we can simplify the condition further to

$$\left(\frac{x+\rho\varepsilon y}{x+\rho y}\right) g(T_F)\left(1-\frac{(x+y)}{K}\right) = r + (1-\rho)\left(\frac{\left(P+B(T_F)y\right)x}{x+\rho y}\right) \tag{11}$$

where we have used the shorthand $x = x(T_F)$ and $y = y(T_F)$.

We conclude that the NPV is maximised (w.r.t rotation length) when the rate of increase in the forest's clear-felled timber value from an additional year of growth equals the discount rate plus the loss in clear-felled timber value from the spread of infection. This formulation shows that the impact of introducing disease on rotation length is effectively to increase the discount rate. It also highlights the trade-off between waiting for trees to grow and infection spreading further.

Similarly, we will now find the optimal thinning time that maximises the NPV, Eq. (4), assuming that the thinning proportion (γ) and rotation time (T_F) are fixed. We derive the first order condition by differentiating Eq. (4) with respect to T_1,

$$\begin{aligned}\frac{\partial \hat{J}}{\partial T_1} &= p_1\gamma\left\{x'(T_1)+\rho y'(T_1)\right\}e^{-rT_1} - rp_1\gamma\left\{x(T_1)+\rho y(T_1)\right\}e^{-rT_1} \\ &\quad + p_2\frac{\partial}{\partial T_1}\left\{x(T_F)+\rho y(T_F)\right\}e^{-rT_F}.\end{aligned} \tag{12}$$

Setting Eq. (12) equal to zero and rearranging after substitution of $x'(T_F)$ and $y'(T_F)$ from Eq. (1) into Eq. (12) gives the optimal thinning time condition

$$\begin{aligned}&\left(\frac{x(T_1)+\rho\varepsilon y(T_1)}{x(T_1)+\rho y(T_1)}\right) g(T_F)\left(1-\frac{x(T_1)+y(T_1)}{K}\right) \\ &= r + (1-\rho)\left(\frac{\left(P+B(T_1)y(T_1)\right)x(T_1)}{x(T_1)+\rho y(T_1)}\right) \\ &\quad - \frac{p_2\frac{\partial}{\partial T_1}\left\{x(T_F)+\rho y(T_F)\right\}e^{-r(T_F-T_1)}}{p_1\gamma\left(x(T_1)+\rho y(T_1)\right)}.\end{aligned} \tag{13}$$

Therefore, we conclude that the NPV is maximised (w.r.t thinning time) when the rate of increase in the thinned timber benefit from an additional year of growth equals the discount rate, plus the loss rate from the spread of infection, minus the discounted change in timber benefit at rotation relative to the thinned timber benefit. Eq. (13) shows that introducing disease has an impact on thinning time similar to the optimal rotation length (Eq. (11)) — disease effectively adds to the discount rate. However, it stresses that the choice of thinning time must account for the impact of thinning on growth and disease dynamics and, therefore, the timber benefit at rotation.

3.1. No disease

We begin with the simplified non-disease version of the model. We can derive this model by setting $P = \beta = 0$ in Eq. (1). Alternatively, by setting $\varepsilon = 1$ in Eq. (1) and $\rho = 1$ in Eq. (5), the disease has no impact on the timber benefit or timber growth. The below equation governs timber dynamics when there is no disease,

$$x'(t) = g(t)x(1-\frac{x}{K}) - h(t). \tag{14}$$

Without disease, thinning extends the optimal clear-felling time compared to the optimal in a clear-felling only regime. This result is a consequence of density-dependent growth, which implies the forest growth rate increases after thinning. We then need to wait longer for the rate of return of timber production to slow and eventually equal the opportunity cost (rate of return of clear-felling and storing cash in the bank). This result can be deduced using the optimal rotation length condition (Eq. (11)), which simplifies to

$$g(T_F)\left(1-\frac{x(T_F)}{K}\right) = r \tag{15}$$

when there is no disease. First, note that the left-hand side of Eq. (15) is a decreasing function of rotation length, T_F, and the right-hand side a constant. Let the optimal rotation length without thinning be T_F^*. If the timber volume without thinning ($\gamma = 0$) is always larger than the timber volume with thinning ($\gamma > 0$) at $t = T_F^*$, i.e., if $x_{\text{no thin}}(T_F^*) \geq x_{\text{thin}}(T_F^*)$, then from Eq. (15) it is clear that optimal rotation with thinning is greater than without. We can show that this is true by solving Eq. (14) using separation of variables for $\gamma = 0$ and $\gamma > 0$ and considering the cases $T_F^* > T_1$ and $T_F^* \leq T_1$. See Appendix A for the details.

Undisturbed growth (no thinning or rotation in Eq. (1)) of the forest is shown in Fig. 1. The density dependence of the forest is highlighted by the optimised thinning and rotation (dotted) line in Fig. 1, as after thinning reduces the volume the growth rate increases.

We highlight that thinning extends the rotation time in Fig. 1, where we compare the two optimised management regimes for the base case economic and ecological parameters (Table 1). The rotation only regime has an optimal rotation length of $T_F \approx 64$, when it is clear-felled. In the optimal thinning and rotation regime, approximately 74% of the total volume is thinned after $T_1 \approx 60$ years, which is just before the optimal rotation in the rotation only regime. Then, after $T_F \approx 89$ years, the plot is clear-felled. We refer to this thinning and rotation strategy as the "disease-free" strategy and use it as a baseline for comparison in later sections of this paper.

We also performed a sensitivity analysis of the optimised thinning and rotation regime to the parameters controlling growth and the price difference between clear-felled and thinned timber. We generally find two optimal strategies; (i) rotation only (no thinning), or (ii) thin $\sim$ 70% of the trees late in the rotation. These parameters have tipping points where the strategy switches between the two strategies. When the growth rate parameters result in quick timber growth, or the price difference between clear-felled and thinned timber is small, thinning is optimal. The optimal strategy switches to no thinning for a large price difference or a small growth rate.

3.2. Disease

3.2.1. No revenue from infected timber

In this section, we investigate the sensitivity of optimal strategies to two epidemiological parameters: the primary infection rate (P) and transmission rate (β). We assume that thinning does not affect transmission ($\delta = 0$) and that the growth rate of infected volume is identical to susceptible ($\varepsilon = 1$); our base case parameter values. With these assumptions the infected volume takes up capacity, limiting the growth of susceptible timber. Therefore, the disease does not impact the density-dependent growth. Instead, we represent a reduced yield by assuming there is no revenue from the infected timber volume ($\rho = 0$). In this scenario, if we fix the strategy in a thinning and rotation regime to be the "disease-free" one, then the total timber volume follows the dashed line in Fig. 1. An increased transmission rate (β) or primary infection rate (P) will speed up the spread of disease and therefore the prevalence of infection at each harvest, Fig. 2.

In Fig. 2(a) and for sensitivity analyses in the following sections of this paper, we set the primary infection $P = 0.0003$, the base case value (Table 1). This value ensures a disease outbreak of some form during a typical rotation (64 years — the optimal without thinning or disease in our model). Furthermore, by sweeping through transmission rates (β) in the range $[0, 0.005]$, we capture a large variation in disease progress curves, see Fig. 6(a). For example, with a low transmission rate $\beta = 0.0005$, the infection spreads very slowly after arrival, and after 60 years less than 5% of the forest has been infected. Then for the transmission rate $\beta = 0.001$, after 60 years approximately 15% of

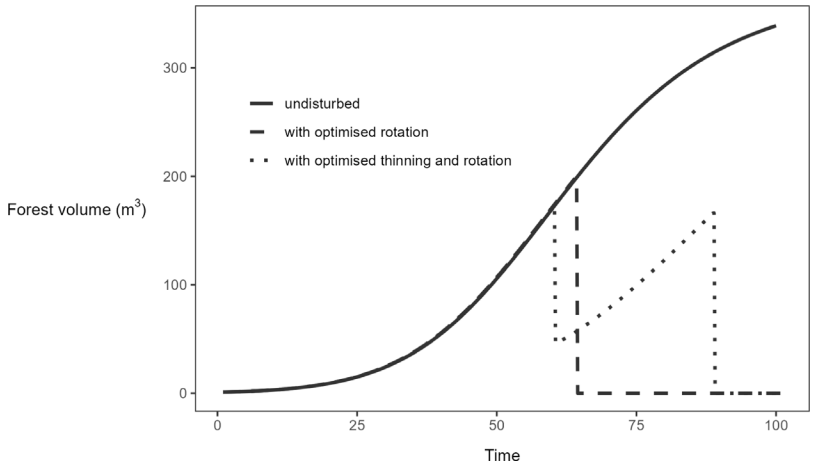

Fig. 1. Timber volume trajectories in absence of disease. Undisturbed timber growth is the thick black line (Eq. (1) with $T_1 = \gamma = 0$, $T_F = \infty$, $\beta = P = 0$ and other parameter values as in Table 1). The dashed line is the timber volume trajectory ($x(t)$ from Eq. (1)) under an optimised clear-felling only management regime (T_1, γ, and T_F given by Eq. (8) for $\beta = P = 0$ and other parameter values as in Table 1). The dotted line is the timber volume trajectory ($x(t)$ from Eq. (1)) under an optimised clear-felling and thinning management regime (solving Eq. (8) for $\beta = P = 0$ and other parameter values as in Table 1).

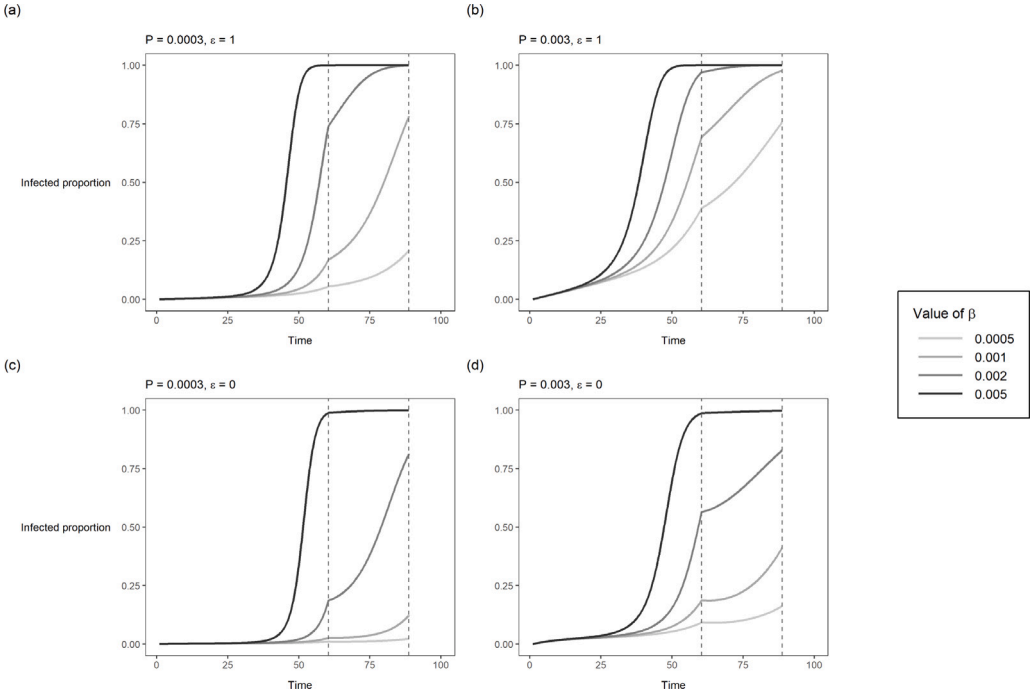

Fig. 2. Disease progress curves under the thinning and clear-felling regime. Epidemiological parameters are varied between panels, but the management regime is fixed to the optimal thinning and clear-felling one in absence of disease. In each panel, the annual cumulative proportion of timber volume infected ($\frac{y(t)}{x(t)+y(t)}$ after solving Eq. (1)) is shown for four values of the transmission rate (β). Each panel shows results for a different combination of the primary infection rate (P) and growth of infected timber relative to susceptible timber (ϵ). The thinning and clear-felling times are the dotted vertical lines in each panel (values shown in Table 1, calculated by solving Eq. (7) for $\beta = P = 0$). All other ecological and economic parameters are given in Table 1.

the forest has been infected. Whereas for higher secondary infection rates, $\beta = 0.002, 0.005$ after 60 years approximately 75% and close to 100% of the forest will be infected.

Increasing the primary infection (P) or transmission rate (β) will shorten the optimal rotation length for each management regime when all other parameters are fixed. To see this, we note that the optimal rotation length condition (Eq. (11)) assuming the thinning proportion (γ) and time (T_1) are fixed and no revenue from infected timber ($\rho = 0$) becomes

$$g(t)\left(1 - \frac{x(T_F) + y(T_F)}{K}\right) = r + \left(P + B(T_F)y(T_F)\right). \tag{16}$$

As the LHS of Eq. (16) is a positive decreasing function of T_F, and the RHS is a positive increasing function of T_F, the LHS and RHS functions will intersect once if plotted. This allows us to deduce the high-level impact of increasing the primary infection (P) or transmission rate (β — which increases $B(T_F)$). Below we use numerical methods to further explore and visualise the interaction between these parameters on the full optimal strategy for each regime.

In a rotation/clear-felling only regime, if the transmission rate (β) is close to zero, a long rotation ($\approx$ 60 years) is optimal, similar to the disease-free length (see Fig. 3(a)). If the external infection pressure or spread rate of disease is higher (increased P or β) then the optimal rotation length (T_F) decreases, as qualitatively shown in Fig. 3(a). Shortening the rotation length allows timber to be salvaged before

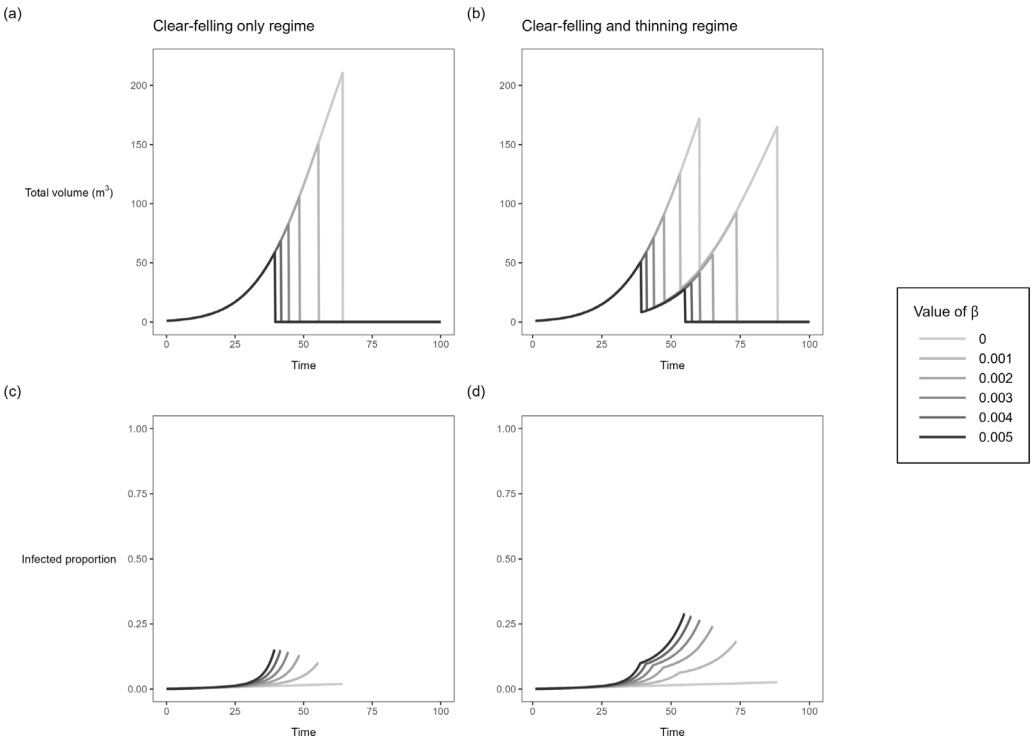

Fig. 3. Impact of transmission rate on optimised management strategies when no revenue comes from infected timber ($\rho = 0$). The top row of panels are the total timber volume trajectories ($x(t) + y(t)$) under the optimised regimes, and the bottom shows the corresponding cumulative proportion of timber infected ($\frac{y(t)}{x(t)+y(t)}$). $x(t)$ and $y(t)$ are given by Eq. (1) with management variables (γ, T_1 and T_F) from either Eq. (8) (rotation only regime) or Eq. (7) (thinning and rotation regime). Darker lines within panels indicate higher values of the transmission rate (β). (a) the total timber volume each year under optimised clear-felling only; (b) the total timber volume each year under optimised thinning and clear-felling; (c) the cumulative proportion of timber infected under optimised clear-felling only; (d) the cumulative proportion of timber infected under optimised thinning and clear-felling.

infection comes (Fig. 3(c)) and destroys its value. The optimal rotation length and maximum NPV are more sensitive to changes in the transmission rate (β) than the primary infection rate (P), see Fig. A.1 in Appendix B which shows the complete breakdown of the optimal strategy in the $\beta - P$ parameter space.

Similarly to the rotation only regime, if the transmission rate is (β) close to zero, it is optimal to follow the "disease-free" strategy with late thinning and long rotation, Fig. 3(b). If the external infection pressure or spread rate of disease is higher (increased P or β), this brings forward the optimal rotation (T_F) and thinning time (T_1) and increases the thinned proportion (γ), compared to the "disease-free" strategy, Fig. 3(b). Salvaging the timber quickly with an early thin and rotation before the infection destroys its value (Fig. 3(d)) becomes optimal (and is intuitive). We refer to this type of strategy as "salvage quickly". The optimal thinning time, proportion, rotation length, and maximum NPV are more sensitive to changes in the transmission rate (β) than the primary infection rate (P), see Fig. A.2 in Appendix B which shows the optimal strategy in the $\beta - P$ parameter space.

Disease causes a severe reduction in maximum NPV for the thinning and rotation regime, particularly for high transmission rate (β). Fig. 4(b) highlights this, where we compare the NPV of using the disease-free strategy (thinning and rotating late) to the optimised strategy for a thinning and rotation regime in the presence of disease. Not shortening rotations when the transmission rate is high ($\beta > 0.002$) will result in immense NPV losses (> £400).

For any fixed value of the primary infection and transmission rates (P and β), the optimal rotation lengths are longer in the thinning and rotation regime compared to those in the rotation-only regime. Thinning times in the thinning and rotation regime occur at roughly the same times as rotation times in the rotation-only regime. To see this, compare Fig. A.1(a) to Fig. A.2(d) in Appendix B, or compare Fig. 3(a) to (b) for an example. The extension is likely due to thinning increasing the forests growth rate, as discussed in Section 3.1, and thinning reducing secondary infection (Fig. 2).

Thinning in combination with clear-felling is always optimal compared to a regime of clear-felling only, Fig. 4(a). Furthermore, thinning is even more profitable when the disease spreads slowly ($\beta < 0.001$ in Fig. 4(a)). Less timber gets destroyed and can be left to grow for longer. Therefore, there can be more time between thinning and clear-felling, allowing the non-thinned trees to grow and exploit the forest's density-dependent growth. A strategy that cannot be applied with clear-felling only. Furthermore, the benefit to including thinning in the management regime decreases with increased transmission rate (β), Fig. 4(a)), becoming very small (< £20) for $\beta > 0.004$. However, comparing Fig. 4(b) (where we compare the NPV of using the disease-free strategy, thinning and rotating late, to the optimised strategy for a thinning and rotation regime in the presence of disease) to Fig. 4(a) in this region ($\beta > 0.004$), we conclude that the largest benefit comes from shortening the rotation, independent of thinning.

3.2.2. *Sensitivity to the revenue from a unit of infected timber relative to uninfected timber*

In Section 3.2.1 we assumed that $\rho = 0$, a worst-case scenario in which timber revenue comes from uninfected timber only. We now investigate the sensitivity of optimal strategies to the effect of infection on timber revenue (i.e., $\rho > 0$). This scenario implicitly represents a smaller impact of infection on yields (through infected tree growth/deaths) or weakened timber being sold at a reduced price. We again assume that thinning does not affect transmission ($\delta = 0$) and that the growth rate of infected volume is identical to susceptible ($\varepsilon = 1$).

Under different combinations of the transmission rate (β) and the infected timber revenue scaling factor (ρ), the optimal strategy (T_F) in a rotation only regime (Eq. (8)) can be categorised into two groups, Fig. 5(a), (c). There is (i) a long rotation used in the disease-free case, and (ii) shorter rotations to salvage timber before infection lessens its value (highlighted in Fig. 5(a), (c)). Fig. A.3 in Appendix B gives a breakdown of the optimal strategy in the $\beta - \rho$ parameter space,

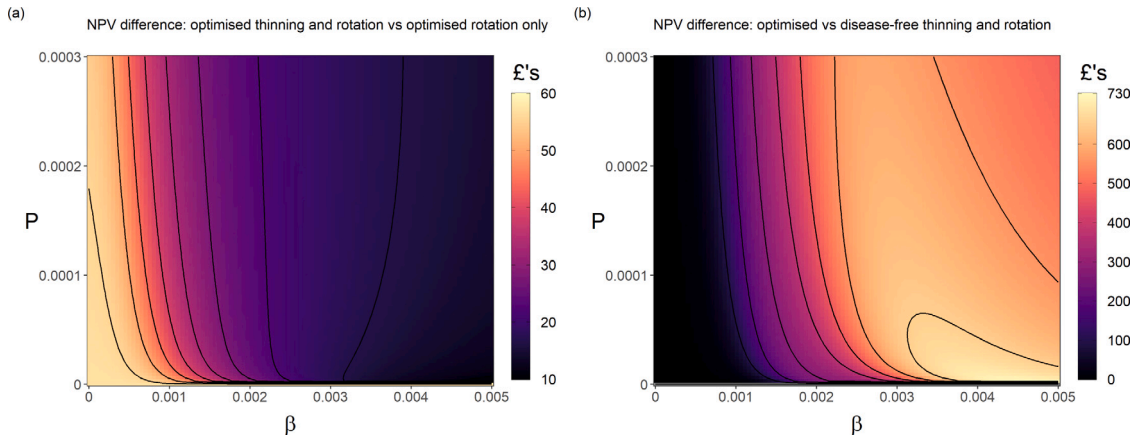

Fig. 4. NPV differences between strategies in a $P-\beta$ parameter space. (a) Difference between the maximum NPV of an optimised thinning and clear-felling regime vs an optimised clear-felling only regime. (b) Difference between using the disease-free strategy (thinning and rotating late) to the optimised strategy for a thinning and rotation regime in the presence of disease. The maximum NPV for optimised thinning and clear-felling is given by substitution of Eq. (7) in Eq. (4), and for clear-felling only by substitution of Eq. (8) in Eq. (4). The disease-free management strategy for thinning and clear-felling is given by solving Eq. (8) for $\beta = P = 0$, keeping all other parameter values as in Table 1. P is the primary infection rate and β is the transmission rate. We assume no revenue comes from infected timber ($\rho = 0$). All other parameter values are given in Table 1.

while Fig. 5(a) and (c) show the optimal strategy at a transect of the transmission rate ($\beta = 0.004$). Along this transect, the two types of strategy that appear in the whole space can be visualised.

Greater damages from infection (lower ρ) typically decrease the optimal rotation length from the disease-free one. The size of the reduction depends on the transmission rate. When the infection spreads slowly (low β), not enough timber is infected for any reduction in timber value to change the optimal rotation length from the disease-free one, Fig. A.3 in Appendix B. When the impact of infection on timber revenue is high ($\rho \leq 0.5$), the optimal length shortens from the disease-free length as the transmission rate (β) increases, Fig. A.3 in Appendix B. The shorter rotation means a lower volume of timber is salvaged, but it is salvaged before infection destroys its value. However, when the impact of infection on timber revenue is lower ($0.5 < \rho < 1$), there is a tipping point with the transmission rate (β); below this value as the transmission rate increases the optimal rotation length decreases, and above this value the optimal rotation length switches back to the optimal disease-free rotation length. The higher the impact of infection on timber revenue (lower $\rho \in (0.5, 1)$), the larger the transmission rate must be for the switch, and the less smooth the switch is. At the switch, the NPV of letting the trees grow larger but more get infected overtakes the NPV of felling a lower yield before they become infected.

Broadly, three types of strategies emerge when we consider the optimal strategy for the thinning and rotation regime (Eq. (7)) under combinations of the transmission rate (β) and the infected timber revenue scaling factor (ρ), Fig. 5(b) (d). Fig. A.4 in Appendix B gives a breakdown of the optimal thinning and rotation strategy in the $\beta - \rho$ parameter space, while Fig. 5(b) and (d) show the optimal strategy at a transect of the transmission rate ($\beta = 0.004$). Along this transect, the three types of strategy that appear in the whole space can be visualised. The first is following the "disease-free" strategy discussed previously. Here, the strategy suggests acting as if there is no disease in the forest — long rotation with late thinning (visualised by the $\rho = 0.85, 1$ lines in Fig. 5(b) (d), and in Fig. 1). This strategy is optimal when either (i) the transmission rate is very low (low β), or (ii) the transmission rate is very high, but infection does not cause much damage (high ρ). The second strategy is "salvage quickly", introduced in Section 3.2.1, and visualised by the $\rho = 0, 0.35$ lines in Fig. 5(b) (d). Here, we thin and rotate earlier. "Salvage quickly" is the optimal strategy when the infection spreads quickly (high β), causing significant damage (low ρ). The final strategy is "best of both worlds", which is optimal when the infection spreads reasonably quickly but causes middling damage to timber ($0.5 \leq \rho \leq 0.8$). The strategy suggests thinning to salvage valuable timber before widespread infection, and then leaving the remaining timber to get infected during a long rotation. The $\rho = 0.45, 0.65, 0.75$ lines in Fig. 5(b) (d) demonstrate this strategy. Note that for any fixed value of the transmission rate and revenue from infected timber (β and ρ), the optimal rotation lengths are longer in the thinning and rotation regime compared to those in the rotation-only regime. To see this, compare Fig. A.1(a) to Fig. A.2(d) in Appendix B, or compare Fig. 5(a) to (b) for an example. The extension is likely due to thinning increasing the forest's growth rate and reducing secondary infection.

The transitions between these different types of optimal strategy suggested in the $\beta - \rho$ parameter space (Fig. A.4 in Appendix B) depend on what the impact of infection on timber revenue (ρ) and transmission rate (β) are. When the impact of infection on timber revenue is high ($\rho \leq 0.4$), the optimal strategy for the thinning and rotation regime changes smoothly with increases in the transmission rate (β), Fig. A.4 in Appendix B. There is a moderate transition from the general "disease-free" to the "salvage quickly" strategy. Optimal rotation and thinning times decrease at a similar rate, and the optimal thinning proportion increases. When the impact of infection on the timber revenue is lower ($\rho > 0.7$), as the transmission rate (β) increases, the optimal rotation and thinning times initially decrease together, and the optimal thinned proportion increases from the "disease-free" values. Then at a tipping point of β (≈ 0.001), this pattern switches. The optimal rotation and thinning time increase together, and the proportion thinned decreases. Furthermore, as β increases further, the rate that the optimal thinning time increases relative to the optimal rotation length slows down, and the optimal strategy becomes a "best of both worlds" type. The impact of infection on timber value (ρ) determines the sensitivity of this switch and the transmission rate where it occurs. When the impact is minor ($\rho > 0.7$), a gradual switch occurs at smaller values of β. When the impact is more significant ($\rho \approx 0.5$), then a tipping point occurs at larger values of the transmission rate (β). At this tipping point, the optimal strategy changes from a "salvage quickly" one (rotating and thinning early) to "best of both worlds" (rotating late but thinning early), visualised by Fig. 5(b) (d).

The NPV differences between the optimised rotation-only regime and the thinning and rotation regime are higher in parameter spaces where the optimal rotation lengths for the thinning and rotation regime are longer (low β, or high β and high ρ), Fig. 6(a). This is because we thin to get an early income, and then exploit the forests density-dependent growth to let the remaining trees grow large. The optimised rotation-only regime cannot offer this option. When the optimal rotation lengths are shorter for both regimes (e.g., high β and low ρ), the density-dependent growth cannot be exploited to the same degree in the optimised thinning and rotation regime (less time between

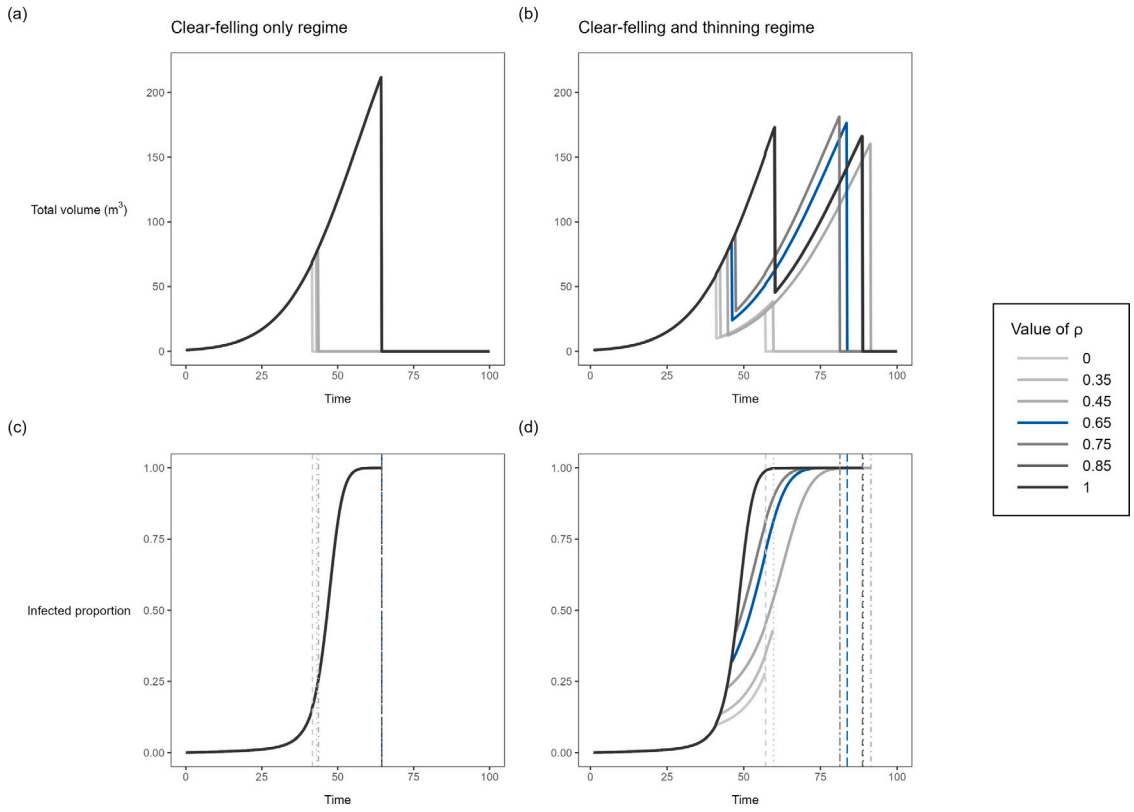

Fig. 5. Impact of transmission rate on optimised management strategies when there is revenue from infected timber ($\rho > 0$). The clear-felling only regime, and the thinning and clear-felling regime were optimised for five different values of the revenue from a unit of infected timber relative to susceptible (ρ) by solving Eqs. (7) and (8). All other parameter values were held at the base case values in Table 1. The top row of panels are the total timber volume trajectories ($x(t) + y(t)$) under the optimised strategies, and the bottom shows the corresponding cumulative proportion of timber infected ($\frac{y(t)}{x(t)+y(t)}$). The vertical lines in the bottom row indicate the clear-felling times from the top row. $x(t)$ and $y(t)$ are given by Eq. (1) with management variables (γ, T_1 and T_F) from either Eq. (8) (rotation only) or Eq. (7) (thinning and rotation). Darker lines within panels indicate higher values of the revenue from a unit of infected timber relative to susceptible (ρ). The blue line highlights the shown value of ρ for which the NPV difference between the thinning and clear-felling regime vs the clear-felling regime is largest (Fig. 6(a)). In panel (a) and (c) the $\rho \geq 0.65$ lines (including blue) are hidden behind the black $\rho = 1$ line. (a) the total timber volume each year under optimised clear-felling only; (b) the total timber volume each year under optimised thinning and clear-felling; (c) the cumulative proportion of timber infected under optimised clear-felling only; (d) the cumulative proportion of timber infected under optimised thinning and clear-felling.

harvests), so the NPV differences are small. The NPV difference between the optimised rotation-only regime and the thinning and rotation regime is highest in the parameter space where the "best of both worlds" thinning and rotation strategy is optimal, see the yellow region in Fig. 6(a). In the centre of this space the optimal strategy for the rotation-only regime switches between rotating early and rotating late (compare $\rho \leq 0.45$ to $\rho \geq 0.65$ lines in Fig. 5(a)). The "best of both worlds" thinning and rotation strategy effectively combines early and late rotation by thinning early and rotating late (blue $\rho = 0.65$ line in Fig. 5(b)); there is not an equivalent strategy for the rotation only regime.

The consequences (NPV losses) of not changing the strategy in the thinning and rotation regime from "disease-free" increase with the transmission rate and the impact of infection on timber revenue, Fig. 6(b). Not shortening the rotation and thinning time when the transmission rate (β) and the impact of infection on timber revenue are high (low ρ) will result in substantial NPV losses (> £500), Fig. 6(b). However, the losses decrease when the transmission rate is exceptionally high as timber is destroyed too quickly compared to the speed at which it grows. When the infection spreads reasonably quickly and causes middling damage to timber ($0.5 \leq \rho \leq 0.8$), it is optimal to use the "best of both worlds" strategy for the thinning and rotation regime. Using this strategy instead of the "disease-free" one in this region provides a slight increase in NPV (≈ £100), Fig. 6(b).

3.2.3. Sensitivity to the impact of thinning on the transmission rate

We now introduce a thinning effect on the transmission rate (setting $\delta > 0$) and investigate the effect on the optimal strategy for the thinning and rotation regime (thinning time, thinning proportion and clear-felling time). We continue to assume that the growth rate of infected volume is identical to susceptible ($\varepsilon = 1$) and no revenue from the infected timber volume ($\rho = 0$).

If the time (T_1) and proportion (γ) of the thinning regime are fixed, increasing the effect of thinning on the transmission rate (δ) will extend the optimal rotation length. This general result follows from the assumption that thinning reduces the transmission rate, $\frac{\partial B(T_F)}{\partial \gamma} < 0$, and can be deduced from Eq. (16) by noting that increasing the thinning effect (δ) reduces $B(T_F)$. Using numerical methods we explored this result further to see how the transmission rate (β) and thinning effect (δ) interact with respect to the full optimal thinning and rotation strategy. We solved Eq. (7) to find the optimised strategy for different combinations of the transmission rate (β) and the thinning effect (δ), holding all other parameters at the base case (Fig. A.7 in Appendix B).

For low transmission rate values (β), the disease does not spread quickly enough and cause enough damage to warrant changing the strategy from "disease-free", i.e., thinning and rotating late to exploit the forest density-dependent growth, Fig. A.7 in Appendix B. Furthermore, when the thinning effect is low ($0 \leq \delta < 2$), increased transmission rate (β) compresses the thinning and rotation times and slightly increases the proportion thinned, as seen previously in Section 3.2.1. However, when the thinning effect is more substantial ($\delta > 2$) and the transmission rate higher ($\beta > 0.001$), increasing the thinning effect (δ) extends the rotation, brings the optimal thinning time forward, and decreases the optimal proportion thinned. The faster infection spreads (higher β), the sooner we thin. The "disease-free" rotation is an upper bound for the rotation length increase.

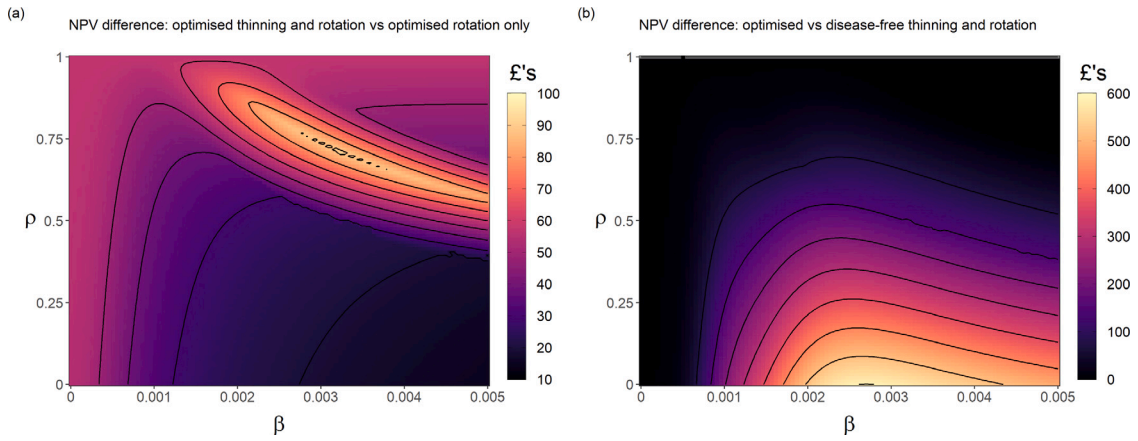

Fig. 6. NPV differences between strategies in a $\rho - \beta$ parameter space. (a) Difference between the maximum NPV of an optimised thinning and clear-felling regime vs an optimised clear-felling only regime. (b) Difference between using the disease-free strategy (thinning and rotating late) to the optimised strategy for a thinning and rotation regime in the presence of disease. The maximum NPV for optimised thinning and clear-felling is given by substitution of Eq. (7) in Eq. (4), and for clear-felling only by substitution of Eq. (8) in Eq. (4). The disease-free management strategy for the thinning and clear-felling regime is given by solving Eq. (8) for $\beta = P = 0$, keeping all other parameter values as in Table 1. ρ is the revenue from a unit of infected timber relative to susceptible, and β is the transmission rate. We assume no revenue comes from infected timber ($\rho = 0$). All other parameter values are given in Table 1.

We conclude that including a strong thinning effect on transmission changes the reason for thinning. Instead of thinning and rotating to get early harvests before infection destroys the value, the optimal strategy suggests thinning early and lightly to protect the final harvest, which can grow larger without being destroyed by the disease. Therefore, the maximum NPV is much higher when there is any thinning effect ($\delta > 0$). The key result of introducing a decline in the transmission rate from thinning bringing the thinning time forward while pushing back the rotation time holds when we change the shape of the decline function. We re-ran the simulation that produced Fig. A.7 using the function $\frac{\beta}{1+\delta\gamma}$ in place of $\beta e^{-\delta\gamma}$ in Eq. (3) and found a similar but less prominent result (not shown).

Furthermore, when infected timber is worthless and the infection spreads quickly ($\beta > 0.0025$), without the thinning impacting the transmission rate, the benefit of thinning and clear-felling over clear-felling is small (Fig. 6(a)). However, comparing Fig. A.7(e) ($\rho = 0$) in Appendix B and Fig. 6(a), when thinning impacts the transmission rate ($\delta > 0$), the benefit in NPV of thinning and clear-felling over only clear-felling alone becomes massive.

3.2.4. Sensitivity to the infected timber growth rate

We now test the sensitivity of the optimised thinning and rotation regime to the growth rate of infected timber relative to susceptible timber (ε). We assume that thinning does not affect transmission ($\delta = 0$) and that revenue from a unit of infected and a unit of susceptible timber volumes are equal ($\rho = 1$). In this scenario, infection disrupts the growth of timber. Furthermore, due to the forests density-dependent growth, as infected timber grows at a reduced rate, susceptible timber volume can grow in its place.

In this scenario where infected timber does not grow at all ($\varepsilon = 0$), if we fix the strategy for the thinning and rotation regime to be the "disease-free" one, then the proportion of volume infected follows Fig. 2(c) and (d). Fixing the epidemiological parameters and comparing (c) and (d) (where epsilon = 0) to (a) and (b) in Fig. 2 (where $\varepsilon = 1$), when the growth rate of infected timber is lower, a larger proportion of the timber volume is susceptible at each harvest.

Under different combinations of the primary (P) and transmission (β) rates, the optimal strategy for the thinning and rotation regime in the $\varepsilon = 0$ scenario (Fig. A.5 in Appendix B) is qualitatively similar to the optimal strategy in the scenario that assumes no revenue from infected timber ($\rho = 0$, Fig. A.2 in Appendix B). However, the NPV's are higher in the $\varepsilon = 0$ scenario. Again, we see that the model is more sensitive to the transmission rate (β) compared to the primary infection rate (P), Fig. A.6 in Appendix B. The optimal rotations shorten and optimal thinned proportion increase from their disease-free values with increases in the transmission rate (β), but at slower rates than when $\rho = 0$. The forests density-dependent growth is responsible for these slower rates. With $\varepsilon = 0$, susceptible trees/volume can grow larger as the infected trees/volume do not grow. Therefore the forest does not need to be clear-felled sooner to recoup costs before infection destroys the value.

Comparing strategies in the $\beta - \varepsilon$ parameter space (Fig. A.6 in Appendix B) to the $\beta - \rho$ parameter space (Fig. A.4 in Appendix B), we see that ε and ρ have somewhat similar effects on the optimal strategy for the thinning and rotation regime, but with some key differences between the effects of ε and ρ. The three types of strategies ("disease-free", "salvage quickly", and a strategy similar to "best of both worlds") outlined in Section 3.2.2 appear in Fig. A.6 in Appendix B. When the infection spreads slowly ($\beta \leq 0.002$), timber is not infected quickly enough for any changes in the infected timber growth rate to alter the optimal strategy from "disease-free" (thinning and rotating later, exploiting density dependence), Fig. A.6 in Appendix B. Similarly, in the $0.8 < \varepsilon \leq 1$ parameter space, it is always optimal to use a "disease-free" type strategy, letting timber become infected under the delayed harvests. The disease does not impact growth enough. If the transmission rate is higher ($\beta > 0.002$), more timber gets infected, and the optimal strategy is much more sensitive to changes in the infected timber growth rate (ε), Fig. A.6 in Appendix B. When the transmission rate (β) is high ($\beta > 0.002$) and the growth rate of infected timber is low ($\varepsilon \leq 0.4$), the optimal rotation length shortens, the optimal thinned proportion increases and thinning occurs slightly later in the rotation, compared to in the "disease-free" type strategy. The strategy becomes a "salvage quickly" type when the growth rate of infected timber is low, and the disease spreads quickly.

Decreasing the infected timber growth rate (ε) has a non-monotonic relationship with optimal rotation length, whereas a reduction in infected timber revenue (ρ) generally always decreases optimal rotation length. When the transmission rate is high ($\beta > 0.003$), reducing the growth rate of infected timber (ε) in the range $0.4 < \varepsilon < 0.8$ gradually decreases the optimal rotation length and thinned proportion, while slightly increasing the timing of the thin relative to the rotation length, Fig. A.6 in Appendix B. Then, at a tipping point of the infected timber growth rate (in $0.4 < \varepsilon < 0.5$), the optimal thinned proportion and rotation length increase with further reduction in $\varepsilon < 0.4$. The increase is more significant for larger transmission rate values and less prominent for the optimal rotation length. Before this switch, little

timber is infected by the thinning time, and far more is infected by rotation time. This is like the "best of both worlds" strategy, seen in the $\beta-\rho$ parameter space (Section 3.2.2 — thinning earlier to salvage before infection, rotating later after infection arrives). The switch highlights how infection spreading slows the overall forest growth and changes the growth dynamics linked to density dependence.

Furthermore, the maximum NPV's are higher in the $\beta-\varepsilon$ parameter space (Fig. A.6 in Appendix B) than in the $\beta-\rho$ parameter space (Fig. A.4 in Appendix B). This is because the forests density-dependent growth allows susceptible timber volume to grow in place of infected volume and infected timber generates revenue ($\rho = 1$). Also, the transitions between strategies are much smoother in the $\beta-\varepsilon$ parameter space compared to the $\beta-\rho$ parameter space. This is related to the objective function's (Eq. (4)) linearity in ρ but not in ε.

4. Discussion

In this paper, we developed a bioeconomic model to determine economically optimal harvesting regimes – in terms of thinning and rotation – of an even-aged plantation under the risk of an invading pest. Using a combination of analytic results and sensitivity analysis, we show that the presence of disease effectively adds to the discount rate in terms of the optimal harvest times (thinning and rotation). However, the complete optimal strategy in the thinning and rotation regime is highly responsive to the anticipated disease characteristics; the transmission rate, the severity of damage caused, the impact on growth and the effect of thinning on disease transmission. The optimal thinning time in our model is when the increase in the thinned timber benefit from an additional year of growth equals the discount rate, plus the loss rate from the spread of infection, minus the discounted change in timber benefit at rotation relative to the thinned timber benefit. Therefore, according to our model, commercial forest managers must decide when to thin to balance harvesting before infection destroys the timber's value, reducing secondary infection and exploiting their forest's density-dependent growth to cultivate target harvests.

Thinning can be used to massively improve the forests' NPV if applied correctly in the presence of disease. We find that adding thinning into the harvesting regime is always optimal, regardless of the disease levels. Timber growth in our model is density-dependent. Thinning, reducing the density and freeing up growing space, exploits this feature to increase the timber benefits produced over the rotation. Lowering the density also has the added benefit of reducing secondary infection. Moreover, when thinning reduces the transmission rate further or presents an opportunity to harvest before a large proportion of the forest is infected, the NPV is improved even further.

Similarly to Macpherson et al. (2016), our model suggests it can be optimal to follow the disease-free thinning and rotation times even when disease prevalence is high. When managers expect infection to cause very little damage to timber value or have a small impact on timber growth, they should continue to thin and rotate late. Additionally, we find that the difference in NPV between the harvesting regime with thinning and one without is largest when long rotations are optimal. Long rotations provide more time to exploit the increased forest growth from thinning.

At a unique balance of middling disease transmission rate and severity of damage from infection, it is optimal to thin early to harvest timber before infection arrives, and leave the remaining trees to become infected and harvested at the disease-free rotation time. Furthermore, we find that the NPV of this strategy is significantly higher than in one without thinning — a rotation only regime can only cut early or late. However, this strategy exists within a narrow parameter space, and more work needs to be done to explore the effect of other parameters (e.g., the discount rate, primary infection, price of thinned timber) on it.

When little revenue is salvageable from infected timber (or infection severely impacts timber growth) and thinning has little impact on the transmission rate, shortening the rotation length from the disease-free length is optimal and has a massive benefit to NPV. Managers should thin and rotate early before infection destroys the forests' value, and the quicker the disease spreads, the sooner they should act. The higher NPV benefit of including thinning in these shorter rotations is small. This finding agrees with an established result in the literature — increased risk of a catastrophic timber loss from natural disasters (storms, fires, severe pest outbreaks) decreases the optimal rotation length (Reed, 1984; Macpherson et al., 2016; Staupendahl and Möhring, 2011; Halbritter et al., 2020). In particular, we confirm that the similar result of Macpherson et al. (2016) holds when (i) thinning is added into a rotation only regime, and (ii) the timber production function is density- and age-dependent. Furthermore, the finding agrees with previous studies that integrated thinning and catastrophic natural risks into Faustmann models (Staupendahl and Möhring, 2011; Halbritter et al., 2020). Staupendahl and Möhring showed that late risks, ones that increase over time, shorten rotations. In our approach, the rate of disease spread increases with age and timber density (which also increases with age) and could be viewed as a late risk. Furthermore, Halbritter et al. (2020) demonstrated that as the expected damage from a catastrophic event increases, optimal rotation lengths decrease.

However, if thinning is expected to reduce the transmission rate significantly, the priority shifts to protect the final harvest. Managers should thin even earlier – slowing the spread of disease – then let the remaining trees grow undisturbed, harvesting them closer to the disease-free rotation time. In this scenario, the NPV of the forest increases significantly, and thinning is the primary driver.

Additionally, including thinning always extends the optimal rotation length compared to that of a rotation-only regime. The optimal rotation length is when the rate of increase in the forest's clear-felled timber value from an additional year of growth equals the discount rate plus the loss in clear-felled timber value from the spread of infection. Including thinning effectively reduces the discount rate because it increases the growth rate of the forest and reduces secondary infection. This result of thinning extending rotation length agrees with some approaches in the literature that built on the Faustmann Model to integrate disease and thinning (Loisel, 2011), but not with others (Halbritter et al., 2020; Petucco and Andrés-Domenech, 2018). In Halbritter et al.'s approach (Halbritter et al., 2020) thinning does not affect the first-order condition of the optimal rotation length. Petucco and Andrés-Domenech (2018) show that including thinning causes a decrease in the optimal rotation length when considering the impact of disease.

In our model, considering disease reduces the optimal rotation length compared to a disease-free scenario. Similarly to Macpherson et al. (2016), the presence of disease effectively adds to the discount rate and so the disease-free rotations are the upper bounds. Petucco and Andrés-Domenech (2018) found the opposite result: increased prevalence of a defoliator pest that slowed tree growth increased the optimal rotation length past the disease-free one. However, when we investigate the sensitivity of our results to the infected timber growth rate without an effect of thinning on transmission (Section 3.2.4), we do find a similar result to theirs. We showed that decreasing the growth rate of infected timber would initially decrease the optimal rotation length when the disease spreads quickly. Then when the impact on growth was particularly severe, the pattern switched and decreasing the growth rate of infected timber further would increase the optimal rotation length towards the disease-free length. This finding highlights a delicate relationship in our model: infection spreading slows the overall forest growth and changes the growth dynamics linked to density dependence. It also highlights the sensitivity of our results to the growth functions used. Furthermore, when the disease has a low impact on timber value, it can be optimal to use a longer rotation length when the spread rate is high compared to if it was low. Therefore, slight

increases in the severity of disease impact do not always add to the interest rate in our approach.

Trees in our investigation are felled indiscriminate of their infection state during thinning. A reasonable extension would be to increase the heterogeneity/complexity of the thinning regime. One modelling approach is to let forest managers bias thinning towards the infected trees. These eradication strategies exist for destructive pathogens such as *Phytophthora ramorum* in the UK, where all trees within a radius around the detected infected ones are felled (O'Hanlon et al., 2018). Another approach is to increase the number of thinning operations during the rotation, even to annual thinning. We also do not consider any unfavourable or unintended impacts of thinning on forest diseases. When trees infected with *Heterobasidian Annosum*, a fungal pathogen that rots trees, are cut down, this exposes the stump, releasing spores and exacerbating the spread (Garbelotto and Gonthier, 2013). In a thinning and rotation regime, as the extent of this exacerbation increases, we could see optimal thinning intensity switch from being nonzero to zero. An understanding of the impact on the entire optimal strategy requires further study.

After thinning, the total timber volume will almost always recover to the carrying capacity (the maximum volume), regardless of the intensity in our model. This may not be a realistic picture, and the link between the volume of individual trees with the volume of the forest is unclear. Our analysis also assumed equal prices for thinned and clear-felled timber, with a fixed price per m^3 for timber. However, as trees grow, their diameters increase alongside their height and volume, and the value of timber grows over time (West, 2014). For example, thinned timber often produces narrow stems sold as wood fuel or firewood. Whereas timber felled later is more mature with a broader set of merchantable applications. We also neglect extraction costs, which could be higher for thinning operations than clear-felling due to economies of scale. As a result, we may have overestimated the net income from thinning, and in turn, the optimal thinning intensities. Having price endogenous to our model, and reflecting individual tree growth, would be an appropriate extension.

We assumed no further planting or harvesting after the single rotation. The main reason behind this is the irreversible nature of tree pests and diseases. A model of multiple rotations would have to incorporate an assumption about what happens to the level of infection between rotations (i.e., if and how the pest/pathogen carries over to the next rotation) (Macpherson et al., 2016). There is significant variation and uncertainty in the ability of pests and diseases to persist after clear-felling (Roberts et al., 2020). Therefore, any assumption we introduce would be highly context and pest/pathogen-specific, making it difficult to draw general conclusions on harvesting strategies. Furthermore, forest managers may deploy different planting schemes (patterns or species) for the next rotation to reduce further disease impact (Roberts et al., 2020). For example, the arrival of Ash Dieback led to a complete ban on the movement and importation of Ash in the UK (Clark and Webber, 2017) . If we introduced an assumption where no disease remained after rotation, this could encourage shorter rotation periods, as fresh timber growing without infection is more valuable. However, this would depend on the rates of forest growth and disease progression. Any leftover disease could increase the proportion of timber infected in future rotations and shorten or increase optimal rotation periods. The outcome would depend on the balance between damage caused by infection and income produced over each rotation. After the stand is clear-felled, we assume it lays bare. Changing the land use after rotation to provide a new source of income could be a reasonable strategy for a forest manager. As shown by Macpherson et al. (2016), including an annual land rent can implicitly capture this opportunity. They show that when the potential income from felling and receiving annual land rent surpasses additional income from leaving the stand to grow, rotation periods decrease.

A forest owner may wish to consider non-timber benefits such as carbon sequestration or recreation in their management strategy. While we have not included these in our model, the work of Macpherson et al. (2017a) provides insight into their potential impact on our results. In their paper, non-timber benefits are internalised into a single rotation Faustmann model with disease risk using a green payment. The green payment counteracts the negative economic effect of disease and incentivises leaving timber unharvested and increasing the optimal rotation length. This effect depends on whether the disease impacts only timber benefits or both timber and non-timber benefits. If non-timber benefits are unaffected, forest owners can be incentivised to never clear-fell their forest. We expect to find similar effects by including non-timber benefits in our model, dependent on how they are generated (e.g., through age, biomass, or forested area). Furthermore, when disease impacts the non-timber benefit and thinning controls disease spread, there may be an additional trade-off with the incentive to thin to protect the non-timber benefits.

5. Conclusion

In this paper, we developed a theoretical and generalisable bio-economic model to determine optimal harvesting strategies under a pathogen or pest invasion. To find the optimal strategy, we maximise the return on investment for a commercial forest manager while accounting for the anticipated interactions between thinning, tree growth and disease progression. Furthermore, we analysed various harvesting regimes through a sensitivity analysis of variable disease conditions. The return on investment for the forest manager is highly sensitive to the type of harvesting strategy employed and the disease characteristics. We investigated the role of thinning in these harvesting strategies and highlighted when its inclusion is vital for forest managers to consider. Our study provides a framework that can help design appropriate forest management strategies in the presence of disease.

Declaration of competing interest

The authors declare that they have no known competing financial interests or personal relationships that could have appeared to influence the work reported in this paper.

Acknowledgements

EM Ph.D. project is funded by the Student Excellence Award, University of Strathclyde. AK contribution was funded by the Scottish Government Strategic Research Programme, Theme 2 project, Disease management options: Insights from comparing forestry and agriculture. EM and AK also acknowledge funding from the NERC project, NE/V019988/1, Learning to adapt to an uncertain future: linking genes, trees, people and processes for more resilient treescapes (newLEAF).

Appendix A. Calculations for the optimal rotation length when there is no disease

When there is no disease, forest dynamics are governed by a single equation,

$$x'(t) = g(t)x(1 - \frac{x}{K}) - h(t) \tag{17}$$

In this section, we will show that

$$x_{\text{no thin}}(T_F^*) \geq x_{\text{thin}}(T_F^*) \tag{18}$$

where T_F^* is the optimal rotation length when there is no disease for a regime without thinning, and $x_{\text{thin}}(t)$ and $x_{\text{no thin}}(t)$ are the timber volumes with and without thinning.

Eq. (17) can be solved analytically using the separation of variables method. With no thinning ($h(t) = 0 \ \forall \ t$ as $\gamma = 0$) we have

$$x_{\text{no thin}}(t) = \frac{K}{\left(\frac{K}{x_0} - 1\right) e^{-\int_0^t g(s)ds} + 1} \tag{19}$$

and when there is thinning

$$x_{\text{thin}}(t) = \begin{cases} x_{\text{no thin}}(t), & 0 \le t \le T_1 \text{ (pre-thinning years)} \\ \dfrac{K}{\left(\frac{K}{(1-\gamma)x_{\text{no thin}}(T_1)} - 1\right) e^{-\int_{T_1}^{t} g(s)ds} + 1}, & t > T_1 \text{ (post-thinning years)} \end{cases} \tag{20}$$

When $T_F^* \le T_1$, after substitution of Eqs. (19) and (20) into Eq. (18), Eq. (18) clearly holds.

When $T_F^* > T_1$, by substitution of $t = T_F^{\text{thin}*}$ into Eqs. (19) and (20) we have

$$x_{\text{thin}}(T_F^*) = \frac{K}{\left(\frac{K}{(1-\gamma)x_{\text{no thin}}(T_1)} - 1\right) e^{-\int_{T_1}^{T_F^*} g(s)ds} + 1} \tag{21}$$

and

$$x_{\text{no thin}}(T_F^*) = \frac{K}{\left(\frac{K}{x_0} - 1\right) e^{-\int_{0}^{T_F^*} g(s)ds} + 1} = \frac{K}{\left(\frac{K}{x_{\text{no thin}}(T_1)} - 1\right) e^{-\int_{T_1}^{T_F^*} g(s)ds} + 1}, \tag{22}$$

and as the RHS of Eq. (21) is a decreasing function of $\gamma \in (0, 1)$ we have Eq. (22) ≥ Eq. (21), i.e., Eq. (18) holds.

Appendix B. Heatmaps showing optimal strategies

See Figs. A.1–A.7 below.

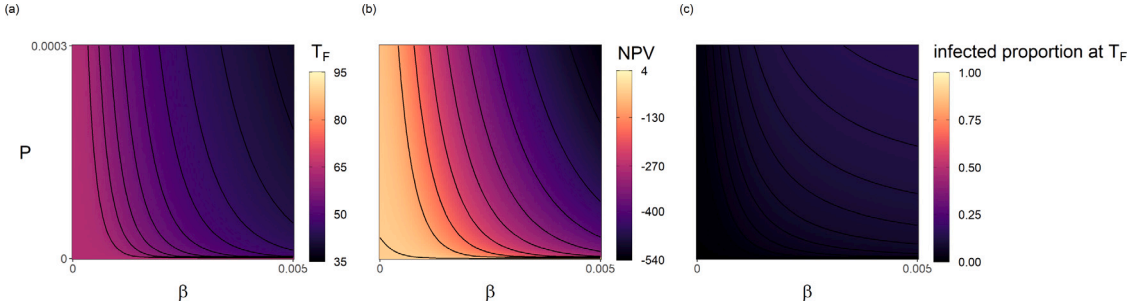

Fig. A.1. Optimal strategy for the rotation only regime in a $P - \beta$ parameter space when there is no revenue from infected timber ($\rho = 0$). The primary infection rate is P, and the transmission rate is β. The optimal strategy for the rotation only regime is found by solving Eq. (8). All other parameter values are given in Table 1. (a) Optimal proportion to thin, γ; (b) Optimal time to thin as a fraction of the rotation length, T_1/T_F; (c) fraction of timber that is infected at the optimal thinning time, $\frac{y(T_1)}{x(T_1)+y(T_1)}$; (d) Optimal rotation length, T_F; (e) NPV under the optimised strategy, $\hat{J}$, given by Eq. (4); (f) fraction of timber that is infected at the rotation time, $\frac{y(T_F)}{x(T_F)+y(T_F)}$.

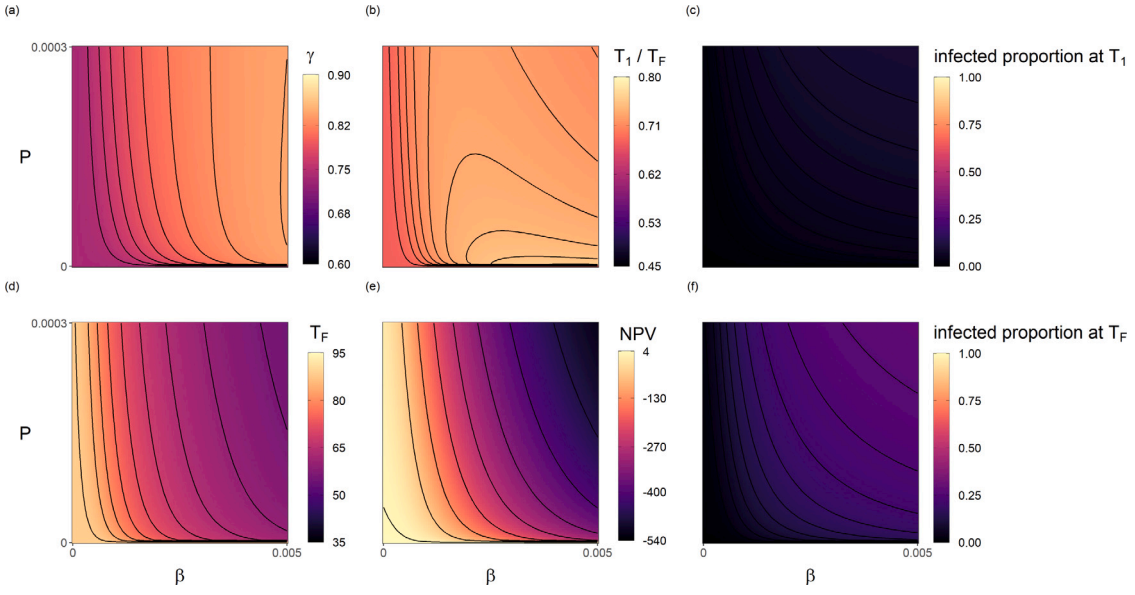

Fig. A.2. Optimal strategy for the thinning and rotation regime in a $P - \beta$ parameter space when there is no revenue from infected timber ($\rho = 0$). The primary infection rate is P, and the transmission rate is β. The optimal strategy for the thinning and rotation regime is found by solving Eq. (7). All other parameter values are given in Table 1. (a) Optimal proportion to thin, γ; (b) Optimal time to thin as a fraction of the rotation length, T_1/T_F; (c) fraction of timber that is infected at the optimal thinning time, $\frac{y(T_1)}{x(T_1)+y(T_1)}$; (d) Optimal rotation length, T_F; (e) NPV under the optimised strategy, $\hat{J}$, given by Eq. (4); (f) fraction of timber that is infected at the rotation time, $\frac{y(T_F)}{x(T_F)+y(T_F)}$.

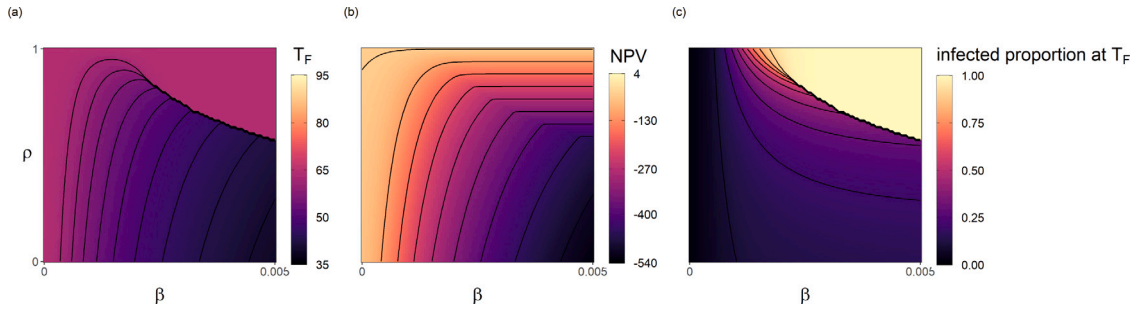

Fig. A.3. Optimal strategy for the rotation only regime in a $\rho - \beta$ parameter space. The revenue from a unit of infected timber relative to susceptible is ρ, and the transmission rate is β. The optimal strategy for the rotation only regime is found by solving Eq. (8). All other parameter values are given in Table 1. (a) Optimal rotation length, T_F; (b) NPV under the optimised strategy, $\hat{J}$, given by Eq. (4); (c) fraction of timber that is infected at the rotation time, $\frac{y(T_F)}{x(T_F)+y(T_F)}$.

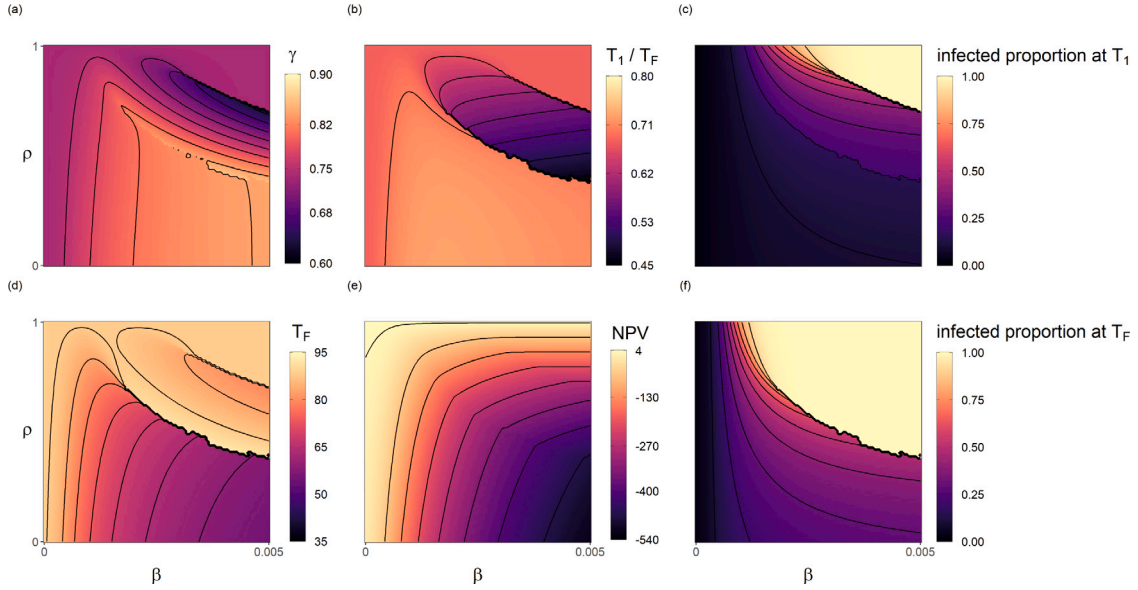

Fig. A.4. Optimal strategy for the thinning and rotation regime in a $\rho - \beta$ parameter space. The revenue from a unit of infected timber relative to susceptible is ρ, and the transmission rate is β. The optimal strategy for the thinning and rotation regime is found by solving Eq. (7). All other parameter values are given in Table 1. (a) Optimal proportion to thin, γ; (b) Optimal time to thin as a fraction of the rotation length, T_1/T_F; (c) fraction of timber that is infected at the optimal thinning time, $\frac{y(T_1)}{x(T_1)+y(T_1)}$; (d) Optimal rotation length, T_F; (e) NPV under the optimised strategy, $\hat{J}$, given by Eq. (4); (f) fraction of timber that is infected at the rotation time, $\frac{y(T_F)}{x(T_F)+y(T_F)}$.

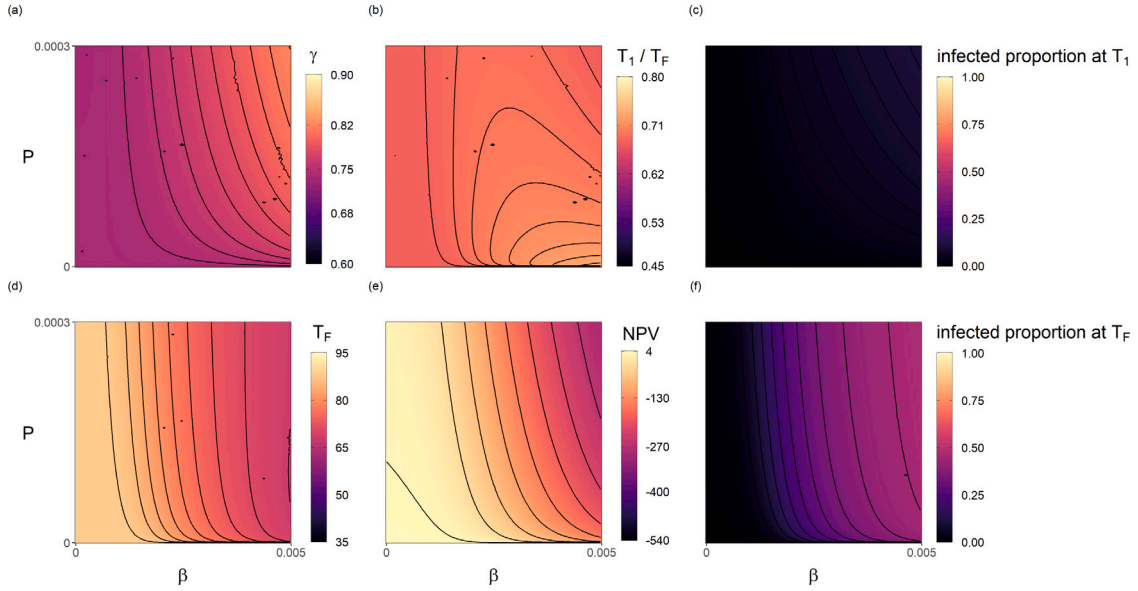

Fig. A.5. Optimal strategy for the thinning and rotation regime in a $P-\beta$ parameter space when infected timber does not grow ($\varepsilon = 0$). The primary infection rate is P, and the transmission rate is β. The optimal strategy for the thinning and rotation regime is found by solving by Eq. (7). Revenue from infected timber is the same value as from susceptible ($\rho = 1$) and all other parameter values are given in Table 1. (a) Optimal rotation length, T_F; (b) NPV under the optimised strategy, $\hat{J}$, given by Eq. (4); (c) fraction of timber that is infected at the rotation time, $\frac{y(T_F)}{x(T_F)+y(T_F)}$.

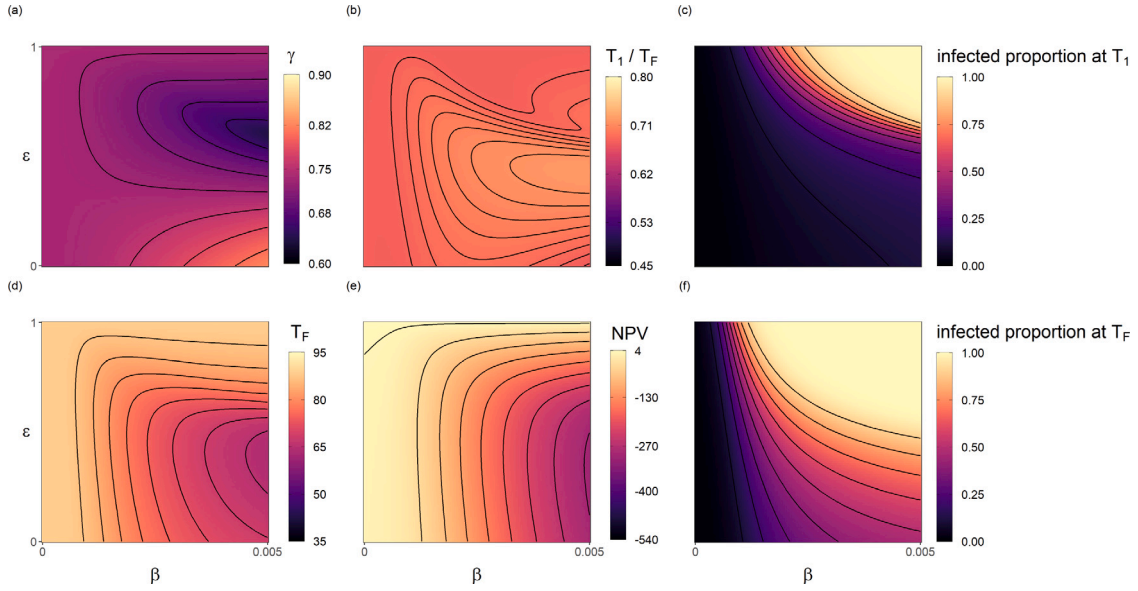

Fig. A.6. Optimal strategy for the thinning and rotation regime in a $\beta-\varepsilon$ parameter space. The transmission rate is β, and growth of infected timber relative to susceptible is ε. The optimal strategy for the thinning and rotation regime is found by solving Eq. (7). All other parameter values are given in Table 1. (a) Optimal proportion to thin, γ; (b) Optimal time to thin as a fraction of the rotation length, T_1/T_F; (c) fraction of timber that is infected at the optimal thinning time, $\frac{y(T_1)}{x(T_1)+y(T_1)}$; (d) Optimal rotation length, T_F; (e) NPV under the optimised strategy, $\hat{J}$, given by Eq. (4); (f) fraction of timber that is infected at the rotation time, $\frac{y(T_F)}{x(T_F)+y(T_F)}$.

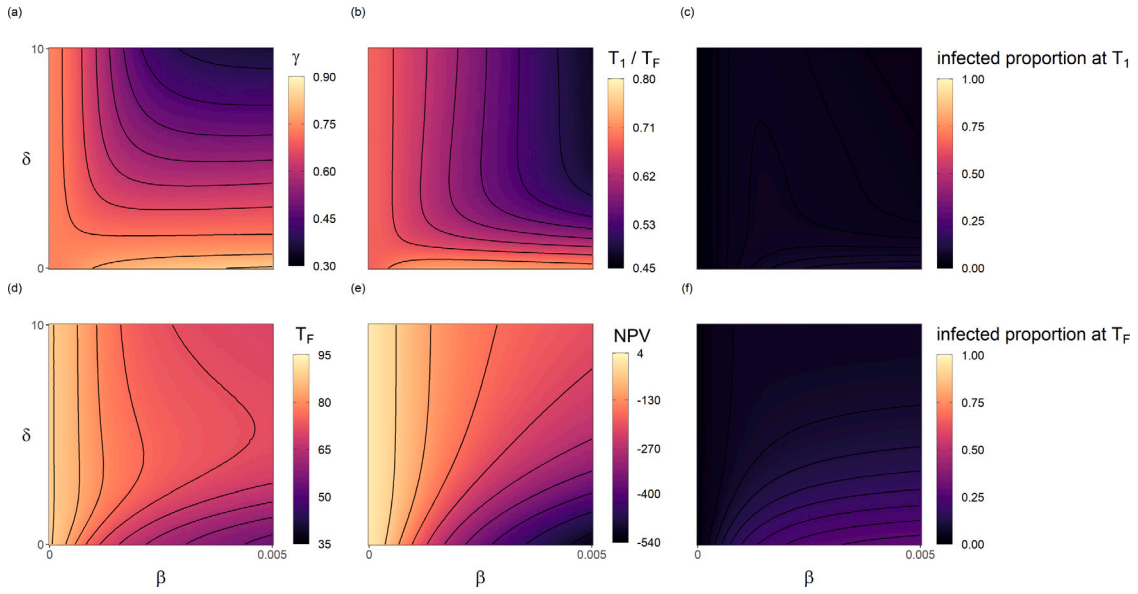

Fig. A.7. Optimal strategy for the thinning and rotation regime in a $\beta - \delta$ parameter space when there is no revenue from infected timber ($\rho = 0$). The transmission rate is β, and δ is the impact of thinning on the transmission rate. The optimal strategy for the thinning and rotation regime is found by solving Eq. (7). All other parameter values are given in Table 1. (a) Optimal proportion to thin, γ; (b) Optimal time to thin as a fraction of the rotation length, T_1/T_F; (c) fraction of timber that is infected at the optimal thinning time, $\frac{y(T_1)}{x(T_1)+y(T_1)}$; (d) Optimal rotation length, T_F; (e) NPV under the optimised strategy, $\hat{J}$, given by Eq. (4); (f) fraction of timber that is infected at the rotation time, $\frac{y(T_F)}{x(T_F)+y(T_F)}$.

References

An, H., Lee, S., Cho, S.J., 2019. The effects of climate change on pine wilt disease in south korea: challenges and prospects. Forests 10 (6), 486, https://doi.org/10.3390/f10060486.

Bauce, É., Fuentealba, A., 2013. Interactions between stand thinning, site quality and host tree species on spruce budworm biological performance and host tree resistance over a 6 year period after thinning. Forest Ecol. Manag. 304, 212–223, https://doi.org/10.1016/J.FORECO.2013.05.008.

Boyd, I.L., Freer-Smith, P.H., Gilligan, C.A., Godfray, H.C.J., 2013. The consequence of tree pests and diseases for ecosystem services. Science 342 (6160), https://doi.org/10.1126/science.1235773.

Boyle, J.R., Tappeiner, J.C., Waring, R.H., Tattersall Smith, C., 2016. Sustainable forestry: Ecology and silviculture for resilient forests. In: Reference Module in Earth Systems and Environmental Sciences. Elsevier, https://doi.org/10.1016/b978-0-12-409548-9.09761-x.

Braby, D., 2022. Timber Price Indices. Forest Research, [Online]. Available: https://www.forestresearch.gov.uk/tools-and-resources/statistics/statistics-by-topic/timber-statistics/timber-price-indices/.

Bulman, L.S., Bradshaw, R.E., Fraser, S., Martín-García, J., Barnes, I., Musolin, D.L., La Porta, N., Woods, A.J., Diez, J.J., Koltay, A., Drenkhan, R., Ahumada, R., Poljakovic-Pajnik, L., Queloz, V., Piškur, B., Doğmuş-Lehtijärvi, H.T., Chira, D., Tomešová-Haataja, V., Georgieva, M., Jankovský, L., Anselmi, N., Markovskaja, S., Papazova-Anakieva, I., Sotirovski, K., Lazarević, J., Adamčíková, K., Boroń, P., Bragança, H., Vettraino, A.M., Selikhovkin, A.V., Bulgakov, T.S., Tubby, K., 2016. A worldwide perspective on the management and control of Dothistroma needle blight. Forest Pathol. 46 (5), 472–488, http://doi.wiley.com/10.1111/efp.12305.

Clark, C.W., De Pree, J.D., 1979. Applied mathematics and optimization a simple linear model for the optimal exploitation of renewable resources. Appl. Math. Optim. 5, 181–196, https://link.springer.com/article/10.1007/BF01442553.

Clark, J., Webber, J., 2017. The ash resource and the response to ash dieback in great britain. In: Vasaitis, R., Enderle, R. (Eds.), Dieback of European Ash (*Fraxinus spp.*): Consequences and Guidelines for Sustainable Management. pp. 228–237, [Online]. Available: https://livingashproject.org.uk/useful-information/.

Cobourn, K.M., Burrack, H.J., Goodhue, R.E., Williams, J.C., Zalom, F.G., 2011. Implications of simultaneity in a physical damage function. J. Environ. Econ. Manag. 62 (2), 278–289. http://dx.doi.org/10.1016/j.jeem.2011.02.002.

Coordes, R., 2014. Optimal Thinning Within the Faustmann Approach. Springer Fachmedien, pp. 1–246, [Online]. Available: https://doi.org/10.1007/978-3-658-06959-9.

Forest Research, 2022a. Dothistroma needle blight (*Dothistroma septosporum*). Forest Research, [Online]. Available: https://www.forestresearch.gov.uk/tools-and-resources/fthr/pest-and-disease-resources/dothistroma-needle-blight/.

Forest Research, 2022b. Pathogens and hosts of Dothistroma needle blight. Forest Research, [Online]. Available: https://www.forestresearch.gov.uk/tools-and-resources/fthr/pest-and-disease-resources/dothistroma-needle-blight/pathogens-and-hosts-of-dothistroma-needle-blight/.

Forestry Commission, 2012. Minimising the Impact of the Great Spruce Bark Beetle. Forestry Commission, [Online]. Available: https://www.forestresearch.gov.uk/publications/minimising-the-impact-of-the-great-spruce-bark-beetle/.

Forestry Commission, 2015. Thinning Control Field Guide. [Online]. Available: https://www.forestresearch.gov.uk/publications/thinning-control-2015/.

Freer-Smith, P.H., Webber, J.F., 2017. Tree pests and diseases: the threat to biodiversity and the delivery of ecosystem services. Biodivers. Conserv. 26, 3167–3181, https://doi.org/10.1007/s10531-015-1019-0.

Garbelotto, M., Gonthier, P., 2013. Biology, epidemiology, and control of *Heterobasidion* species worldwide. Annu. Rev. Phytopathol. 51, 39–59, https://doi.org/10.1146/annurev-phyto-082712-102225.

Halbritter, A., Deegen, P., 2015. A combined economic analysis of optimal planting density, thinning and rotation for an even-aged forest stand. Forest Policy Econ. 51, 38–46, https://doi.org/10.1016/j.forpol.2014.10.006.

Halbritter, A., Deegen, P., Susaeta, A., 2020. An economic analysis of thinnings and rotation lengths in the presence of natural risks in even-aged forest stands. Forest Policy Econ. 118, http://dx.doi.org/10.1016/j.forpol.2020.102223.

Hlásny, T., Krokene, P., Liebhold, A., Montagné-Huck, C., Müller, J., Qin, H., Raffa, K., Schelhaas, M.-J., Seidl, R., Svoboda, M., 2019. Living with bark beetles: Impacts, outlook and management options. In: From Science to Policy 8. European Forest Institute, [Online]. Available: https://doi.org/10.36333/fs08.

Kerr, G., Haufe, J., 2011. Thinning Practice: A Silvicultural Guide. Forestry Commission, [Online]. Available: https://www.forestresearch.gov.uk/publications/thinning-practice-a-silvicultural-guide/.

Klapwijk, M.J., Hopkins, A.J.M., Eriksson, L., Pettersson, M., Schroeder, M., Lindelöw, Å., Rönnberg, J., Keskitalo, E.C.H., Kenis, M., 2016. Reducing the risk of invasive forest pests and pathogens: combining legislation, targeted management and public awareness. Ambio 45, 223–234, https://doi.org/10.1007/s13280-015-0748-3.

Kleczkowski, A., Hoyle, A., McMenemy, P., 2019. One model to rule them all? Modelling approaches across OneHealth for human, animal and plant epidemics. Philos. Trans. R. Soc. 374 (1755), http://dx.doi.org/10.1098/rstb.2018.0255.

Loisel, P., 2011. Faustmann rotation and population dynamics in the presence of a risk of destructive events. J. Forest Econ. 17 (3), 235–247. http://dx.doi.org/10.1016/j.jfe.2011.02.001.

Macpherson, M.F., Kleczkowski, A., Healey, J.R., Hanley, N., 2016. The effects of disease on optimal forest rotation: A generalisable analytical framework. Environ. Resour. Econ. 70, 565–588, https://doi.org/10.1007/s10640-016-0077-4.

Macpherson, M.F., Kleczkowski, A., Healey, J.R., Hanley, N., 2017a. Payment for multiple forest benefits alters the effect of tree disease on optimal forest rotation length. Ecol. Econom. 134, 82–94, https://doi.org/10.1016/j.ecolecon.2017.01.008.

Macpherson, M.F., Kleczkowski, A., Healey, J.R., Quine, C.P., Hanley, N., 2017b. The effects of invasive pests and pathogens on strategies for forest diversification. Ecol. Model. 350, 87–99, https://doi.org/10.1016/j.ecolmodel.2017.02.003.

Mäkinen, H., Isomäki, A., 2004. Thinning intensity and growth of norway spruce stands in finland. Forestry 77 (4), 349–364. http://dx.doi.org/10.1093/FORESTRY/77.4.349.

Marzano, M., Fuller, L., Quine, C.P., 2017. Barriers to management of tree diseases: Framing perspectives of pinewood managers around Dothistroma Needle Blight. J. Environ. Manag. 188, 238–245, https://doi.org/10.1016/J.JENVMAN.2016.12.002.

Matthews, R.W., Jenkins, T.A.R., Mackie, E.D., Dick, E.C., 2016. Forest Yield: A Handbook on Forest Growth and Yield Tables for British Forestry. Forestry Commission, [Online]. Available: https://www.forestresearch.gov.uk/publications/forest-yield-a-handbook-on-forest-growth-and-yield-tables-for-british-forestry/.

Mullett, M.S., Tubby, K.V., Webber, J.F., Brown, A.V., 2016. A reconsideration of natural dispersal distances of the pine pathogen *Dothistroma septosporum*. Plant Pathol. 65 (9), 1462–1472, https://doi.org/10.1111/ppa.12522.

Office for National Statistics, 2020. Woodland Natural Capital Accounts Ecosystem Services for England, Scotland, Wales and Northern Ireland, 2020. Office for National Statistics, [Online]. Available: https://www.ons.gov.uk/economy/environmentalaccounts/bulletins/woodlandnaturalcapitalaccountsuk/ecosystemservicesforenglandscotlandwalesandnorthernireland2020#woodland-natural-capital-accounts-ecosystem-services-data.

O'Hanlon, R., Choiseul, J., Brennan, J.M., Grogan, H., 2018. Assessment of the eradication measures applied to *Phytophthora ramorum* in irish *Larix kaempferi* forests. Forest Pathol. 48 (1), http://dx.doi.org/10.1111/efp.12389.

Petucco, C., Andrés-Domenech, P., 2018. Land expectation value and optimal rotation age of maritime pine plantations under multiple risks. J. Forest Econ. 30 (1), 58–70. http://dx.doi.org/10.1016/j.jfe.2018.01.001.

Potter, C., Urquhart, J., 2017. Tree disease and pest epidemics in the Anthropocene: A review of the drivers, impacts and policy responses in the UK. Forest Policy Econ. 79, 61–68. http://dx.doi.org/10.1016/J.FORPOL.2016.06.024.

Quine, C., Marzano, M., Fuller, L., Dandy, N., Barnett, J., Brandon, G., Jones, G., Porth, E., Price, C., 2014. Social and Economic Analyses of Dothistroma Needle Blight Management. Forest Research, [Online]. Available: https://www.forestresearch.gov.uk/publications/social-and-economic-analyses-of-dothistroma-needle-blight-management/.

Ramsfield, T.D., Bentz, B.J., Faccoli, M., Jactel, H., Brockerhoff, E.G., 2016. Forest health in a changing world: Effects of globalization and climate change on forest insect and pathogen impacts. Forestry 89 (3), 245–252, https://doi.org/10.1093/forestry/cpw018.

Reed, W.J., 1984. The effects of the risk of fire on the optimal rotation of a forest. J. Environ. Econ. Manag. 11 (2), 180–190, https://doi.org/10.1016/0095-0696(84)90016-0.

Roberts, M., Gilligan, C.A., Kleczkowski, A., Hanley, N., Whalley, A.E., Healey, J.R., 2020. The effect of forest management options on forest resilience to pathogens. Front. For. Glob. Chang. 3, https://doi.org/10.3389/ffgc.2020.00007.

Samuelson, P.A., 1976. Economics of forestry in an evolving society. Economic Enquiry 14 (4), https://doi.org/10.1111/j.1465-7295.1976.tb00437.x.

Scottish Forestry, Dothistroma needle blight in Scotland. Scottish Forestry, [Online]. Available: https://forestry.gov.scot/sustainable-forestry/tree-health/tree-pests-and-diseases/dothistroma-needle-blight.

Staupendahl, K., Möhring, B., 2011. Integrating natural risks into silvicultural decision models: A survival function approach. Forest Policy Econ. 13 (6), 496–502. http://dx.doi.org/10.1016/j.forpol.2011.05.007.

Sturrock, R.N., Frankel, S.J., Brown, A.V., Hennon, P.E., Kliejunas, J.T., Lewis, K.J., Worrall, J.J., Woods, A.J., 2011. Climate change and forest diseases. Plant Pathol. 60 (1), 133–149, https://doi.org/10.1111/j.1365-3059.2010.02406.x.

Tahvonen, O., 2016. Economics of rotation and thinning revisited: The optimality of clearcuts versus continuous cover forestry. Forest Policy Econ. 62, 88–94, https://doi.org/10.1016/j.forpol.2015.08.013.

West, P.W., 2014. Growing Plantation Forests, 2 Springer Cham, [Online]. Available: https://doi.org/10.1007/978-3-319-01827-0.

Zeide, B., 2001. Thinning and growth: a full turnaround. Journal of Forestry 99 (1), 20–25, https://doi.org/10.1093/jof/99.1.20.